OPEN

Sema3F (Semaphorin 3F) Selectively Drives an Extraembryonic Proangiogenic Program

Donatella Regano,* Alessia Visintin,* Fabiana Clapero, Federico Bussolino, Donatella Valdembri, Federica Maione,† Guido Serini,† Enrico Giraudo†

Objective—Molecular pathways governing blood vessel patterning are vital to vertebrate development. Because of their ability to counteract proangiogenic factors, antiangiogenic secreted Sema3 (class 3 semaphorins) control embryonic vascular morphogenesis. However, if and how Sema3 may play a role in the control of extraembryonic vascular development is presently unknown.

Approach and Results—By characterizing genetically modified mice, here, we show that surprisingly Sema3F acts instead as a selective extraembryonic, but not intraembryonic proangiogenic cue. Both in vivo and in vitro, in visceral yolk sac epithelial cells, Sema3F signals to inhibit the phosphorylation-dependent degradation of Myc, a transcription factor that drives the expression of proangiogenic genes, such as the microRNA cluster 17/92. In *Sema3f*-null yolk sacs, the transcription of Myc-regulated microRNA 17/92 cluster members is impaired, and the synthesis of Myc and microRNA 17/92 foremost antiangiogenic target Thbs1 (thrombospondin 1) is increased, whereas Vegf (vascular endothelial growth factor) signaling is inhibited in yolk sac endothelial cells. Consistently, exogenous recombinant Sema3F inhibits the phosphorylation-dependent degradation of Myc and the synthesis of Thbs1 in mouse F9 teratocarcinoma stem cells that were in vitro differentiated in visceral yolk sac epithelial cells. *Sema3f*$^{-/-}$ mice placentas are also highly anemic and abnormally vascularized.

Conclusions—Sema3F functions as an unconventional Sema3 that promotes extraembryonic angiogenesis by inhibiting the Myc-regulated synthesis of Thbs1 in visceral yolk sac epithelial cells.

Visual Overview—An online visual overview is available for this article. **(*Arterioscler Thromb Vasc Biol*. 2017;37: 1710-1721. DOI: 10.1161/ATVBAHA.117.308226.)**

Key Words: angiogenesis modulating agents ■ mice ■ myc ■ semaphorins ■ thrombospondins ■ yolk sac

Effective delivery of oxygen and nutrients is mandatory for proper development of mammalian embryos.[1] Although initially supported by molecular diffusion only, around day 8 of gestation (E8), the mouse embryo starts relying in full on blood circulation to further develop. By this time, heart starts beating and extraembryonic yolk sac blood islands, that is, mesoderm-derived clusters of hematopoietic cells surrounded by a layer of endothelial cells (EnCs), coalesce to form a vascular network filled with large nucleated primitive erythroblasts.[2] This allows vital molecules to diffuse from the maternal blood, which is contained in giant trophoblast cell-lined uterine sinuses, into visceral yolk sac blood vessels that directly connect to the embryonic vasculature. Between E12.5 and E14.5, the mature chorioallantoic placenta progressively replaces the yolk sac as main nutrient exchange organ supporting the development of the mouse embryo.[3]

Large embryonic blood vessels and the vasculature of several embryonic organs and extraembryonic yolk sac initially arise by vasculogenesis, namely, the differentiation of angioblasts into EnCs that self-assemble in a homogeneously-sized primitive vascular plexus.[1] The latter is then remodeled by angiogenesis into a hierarchically sized mature vascular tree that facilitates and optimizes the distribution of blood.[1] In this context, EnC mechanosensitive adhesion receptors translate blood fluid shear traction forces into biochemical signals that allow vascular remodeling and maturation.[4] Although it is well established that extraembryonic EnCs do not contribute to intraembryonic blood vessels, the molecular mechanisms that differentially regulate yolk sac and embryonic vascularization are poorly defined.[1]

Sema3 (class 3 semaphorins) are secreted guidance cues that in the developing embryo signal through the cytosolic

Received on: June 28, 2016; final version accepted on: July 7, 2017.

From the Candiolo Cancer Institute, Fondazione del Piemonte per l'Oncologia, Istituto di Ricovero e Cura a Carattere Scientifico, Candiolo, Torino, Italy (D.R., A.V., F.C., F.B., D.V., F.M., G.S., E.G.); Department of Science and Drug Technology, University of Torino, Italy (D.R., A.V., F.M., E.G.); and Department of Oncology, University of Torino School of Medicine, Candiolo, Italy (F.C., F.B., D.V., G.S.).

*These authors contributed equally to this article as first authors.

†These authors contributed equally to this article as senior authors.

The online-only Data Supplement is available with this article at http://atvb.ahajournals.org/lookup/suppl/doi:10.1161/ATVBAHA.117.308226/-/DC1.

Correspondence to Enrico Giraudo, PhD, Laboratory of Transgenic Mouse Models, Candiolo Cancer Institute – Fondazione del Piemonte per l'Oncologia, Istituto di Ricovero e Cura a Carattere Scientifico, Torino, Italy, E-mail enrico.giraudo@ircc.it; or Guido Serini, MD, PhD, Laboratory of Cell Adhesion Dynamics, Candiolo Cancer Institute – Fondazione del Piemonte per l'Oncologia, Istituto di Ricovero e Cura a Carattere Scientifico, Torino, Italy, E-mail guido.serini@ircc.it

Nonstandard Abbreviations and Acronyms	
CK8/18	cytokeratin 8/18
EnCs	endothelial cells
EpCs	epithelial cells
Fbw7	F-box and WD repeat domain-containing 7
GAP	GTPase-activating protein
PYS	parietal yolk sac
rSEMA3F	recombinant semaphorin 3F
SNAIL1	snail family transcriptional repressor 1
Thbs1	thrombospondin 1
VYS	visceral yolk sac

GAP (GTPase-activating protein) domain of Plexin receptors[5] to inhibit R-Ras, M-Ras, and Rap1, 3 small GTPases that are crucial positive regulators of integrin-mediated cell adhesion in different cell types, EnC included.[6,7] The chemorepulsive activity of Sema3A[8–10] and Sema3E[11] was previously reported to control the vascular patterning in chick, zebrafish, and mouse embryos.[12] In addition, thanks to their ability to inhibit angiogenesis, both Sema3A and Sema3E exert an effective anticancer activity.[13,14] Similarly, Sema3F was also found to display powerful antiangiogenic and antitumor effects[13,14]; however, if and how Sema3F may play a role in embryonic vascular development is unknown. Surprisingly, at odds with the antiangiogenic function of all other Sema3 proteins, here we unveil how Sema3F drives a Myc-dependent proangiogenic program that is selectively restricted to the extraembryonic vasculature. In addition to shedding light on the molecular mechanisms that selectively drive extraembryonic but not embryonic blood vessel formation, our findings also suggest how an aberrant expression of Sema3F might be involved in placenta vascular malformations.

Materials and Methods

Materials and Methods are available in the online-only Data Supplement.

Results

Targeted Disruption of Mouse *Sema3f* Gene Results in Partially Penetrant Embryonic Lethality but Does Not Control Embryonic Vascular Development

To understand whether Sema3F may control both embryonic and postnatal mouse development, we characterized and compared *Sema3f*- and, for control purposes, *Sema3a*-null mice.[8] Heterozygous *Sema3a* and *Sema3f* mice were phenotypically normal and fertile. As expected,[8] the percentage of born *Sema3a*-null mice was also much lower than the Mendelian ratio (5.7% $Sema3a^{-/-}$, 39.1% $Sema3a^{+/+}$, 55.2% $Sema3a^{+/-}$; n=460). Similarly, Walz et al[15] already described that $Sema3f^{-/-}$ mice were born significantly less (14%) than that predicted by Mendelian ratio. As shown in Table 1, we confirmed that the frequency of born *Sema3f*-knockout pups is indeed lower than expected (5.7% $Sema3f^{-/-}$, 29.4% $Sema3f^{+/+}$, 64.9% $Sema3f^{+/-}$; n=465). The higher embryonic lethality we observed in our $Sema3f^{-/-}$ mice compared with that reported by Walz et al[15] might be likely because of differences in the percentage of C57Bl/6 and 129P2/OlaHsd genetic backgrounds between the 2 colonies (see Materials and Methods and Figure I in the online-only Data Supplement). Thus, similarly to $Sema3a^{-/-}$ mice, most of *Sema3f*-null mice also die in utero.

To assess the timing of embryolethality, we genotyped embryos collected at different developmental stages. Between E9.5 and E10.5, a clear significant decrease in *Sema3f*- and *Sema3a*-null embryos emerged. In particular, the *Sema3f*-null embryos were 19.6% at E9.5 (n=249) and 13.5% at E10.5 (n=81), whereas those of *Sema3a*-null embryos were 18.6% at E9.5 (n=285) and 15.2% at E10.5 (n=105). No gross phenotypic differences were present in the few outliving *Sema3f*- or *Sema3a*-knockout mice. However, as previously reported,[16] if matched with wild-type mice of the same litter, 3-week-old $Sema3a^{-/-}$ mice were smaller in size, their weight was halved, and they had difficulty maintaining an upright posture.

Sema3A signaling was previously reported to control vascular morphogenesis in zebrafish,[9] chick,[10] and mouse embryos.[8,17–19] We hence investigated whether, similar to Sema3A, Sema3F may also regulate mouse embryonic angiogenesis. We examined by fluorescence confocal microscopy the vasculature of whole-mount endomucin-stained wild type (Figure 1A through 1D), *Sema3f*-null (Figure 1F through 1I), and *Sema3a*-null (Figure 1K through 1N) embryos at E9.5. Compared with control littermates (Figure 1E), *Sema3f*- knockout embryos (Figure 1J) displayed retarded growth (E9.5 wild-type embryos: 21.2±0.5 somites; E9.5 $Sema3f^{-/-}$ embryos: 18.8±0.5 somites; Table 2) but not major vascular defects (Figure 1A through 1D and 1F through 1I). In agreement with previous studies[8] and differently from

Table 1. Genotypes of the Offspring Generated From *Sema3f* and *Sema3a* Heterozygous Intercrosses on a C57BL/6 Background

Sema3f					*Sema3a*				
	Total	+/+	+/−	−/−		Total	+/+	+/−	−/−
Term pups	465	29.4% (137)	64.9% (302)	5.7% (26)	Term pups	460	39.1% (180)	55.2% (254)	5.7% (26)
E9.5	249	27.7% (69)	32.1% (80)	19.6% (49)	E9.5	285	30.2% (86)	51.2% (146)	18.6% (53)
E10.5	81	40.7% (33)	45.6% (37)	13.5% (11)	E10.5	105	32.4% (34)	52.4% (55)	15.2% (16)

Heterozygous *Sema3a* and *Sema3f* mice were intercrossed, and the progeny was analyzed. Only 5.7% adult knockout mice were observed after genotyping the offspring of both $Sema3f^{+/-}$ (n=465) and $Sema3a^{+/-}$ (n=460) mating, respectively. Timed mating revealed an embryonic lethality between E9.5 and E10.5 in both *Sema3f* and *Sema3a* mutants. A percentage of 19.6 (n=249) at E9.5 and 13.5 (n=81) at E10.5 was observed in the progeny of *Sema3f* intercrosses and a percentage of 18.6 (n=285) at E9.5 and 15.2 (n=105) at E10.5 was observed in the progeny of *Sema3a*. Sema3 indicates class 3 semaphorin.

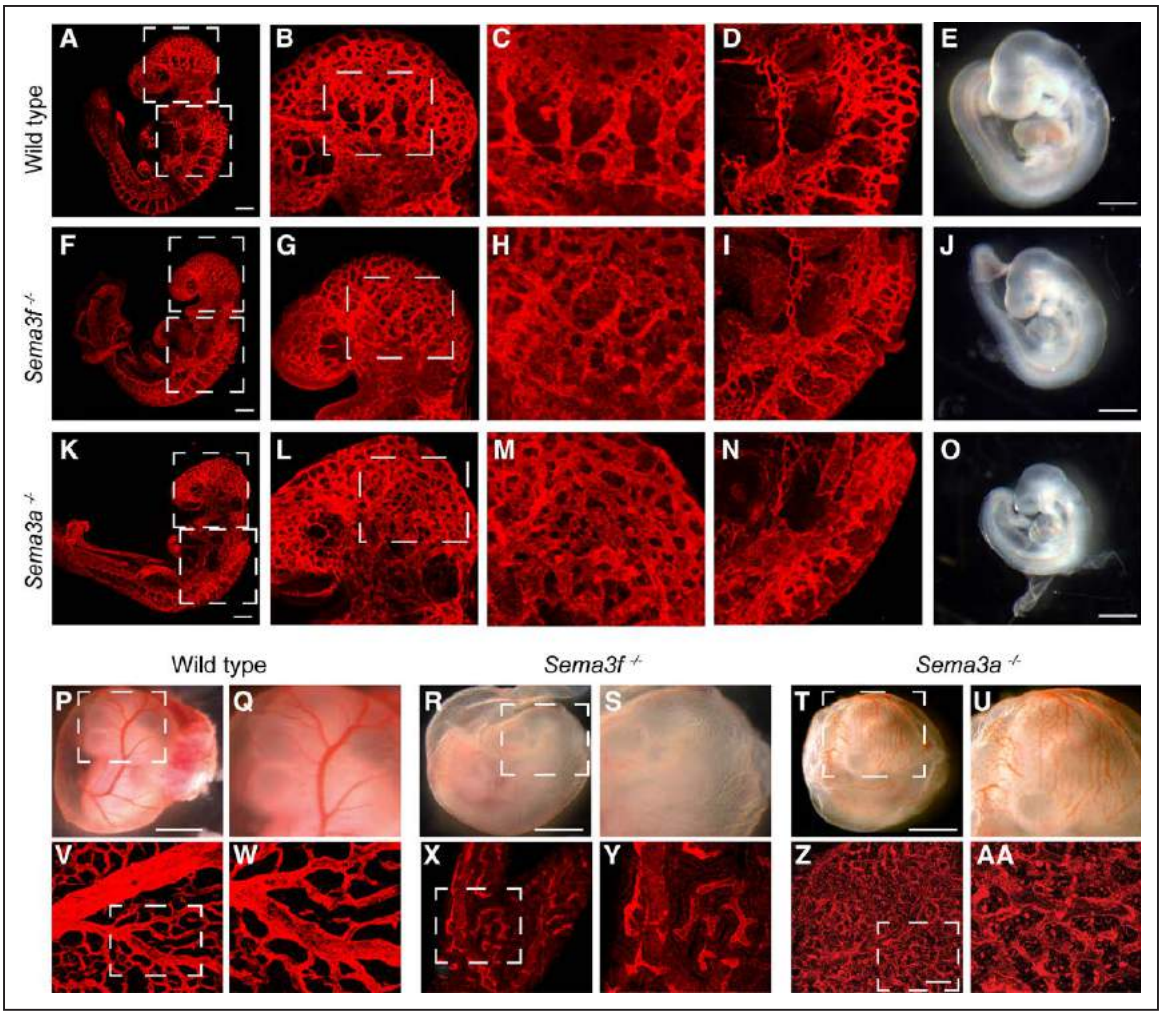

Figure 1. Sema3 (class 3 semaphorin)-A is necessary for embryonic angiogenic remodeling, whereas Sema3F is required for yolk sac blood vessel formation. Whole-mount endomucin stained E9.5 wild-type (**A** through **D**), *Sema3f*$^{-/-}$ (**F** through **I**), and *Sema3a*$^{-/-}$ (**K** through **N**) embryos. The cephalic plexus of wild-type (**B** and **C**) and *Sema3f*$^{-/-}$ (**G** and **H**) but not *Sema3a*$^{-/-}$ (**L** and **M**) embryos is remodeled to give rise to easily distinguishable cephalic veins. The cephalic perineural vascular plexus develops through remodeling of the dorsal longitudinal anastomotical vessel in wild-type (**D**) and *Sema3f*$^{-/-}$ (**I**) but not in *Sema3a*$^{-/-}$ embryos (**N**). **E**, **J**, and **O**, Stereomicroscopic analyses reveals how, when compared with age-matched wild-type embryos (**E**), the development of both *Sema3f*$^{-/-}$ (**J**) and *Sema3a*$^{-/-}$ (**O**) E9.5 embryos is delayed. Developmental delay is more severe in *Sema3a*$^{-/-}$ (**O**) than that in *Sema3f*$^{-/-}$ (**J**) embryos. **B**, **G**, and **L**, Magnifications of the top boxed areas in (**A**), (**F**), and (**K**), respectively. **C**, **H**, and **M**, Magnifications of the boxed areas in (**B**), (**G**), and (**L**), respectively. **D**, **I**, and **N**, Magnifications of the bottom boxed areas in (**A**), (**F**), and (**K**), respectively. Scale bars, 300 μm (**A**, **F**, and **K**) and 100 μm (**E**, **J**, and **O**). Stereomicroscopy (**P** through **U**) and endomucin-staining confocal microscopy (**V** through **AA**) analyses of E10.5 wild-type (**P**, **Q**, **V**, and **W**), *Sema3f*$^{-/-}$ (**R**, **S**, **X**, and **Y**) and *Sema3a*$^{-/-}$ (**T**, **U**, **Z**, and **AA**) yolk sacs. When compared with wild-type yolk sacs (**P**, **Q**, **V**, and **W**), a dramatic decrease in blood vessels is observed in *Sema3f*$^{-/-}$ yolk sacs (**R**, **S**, **X**, and **Y**), while a poorly remodeled primary capillary plexus and the persistence of some blood islands characterize *Sema3a*$^{-/-}$ (**T**, **U**, **Z**, and **AA**) yolk sacs. **Q**, **S**, **U**, **W**, **Y**, and **AA**, Magnifications of (**P**), (**R**), (**T**), (**V**), (**X**), and (**Z**), respectively. Scale bars, 100 μm (**P**, **R**, and **T**) and 150 μm (**V**, **X**, and **Z**).

Sema3f-null embryos (Figure 1J), *Sema3a*-knockout embryos (Figure 1O) displayed an even stronger growth retardation (E9.5 *Sema3a*$^{-/-}$ embryos: 17±1.2 somites, n=7; Figure 1O) that was associated with angiogenic remodeling defects (Figure 1K through 1N). The cephalic plexus of wild-type (Figure 1B and 1C) and *Sema3f*$^{-/-}$ (Figure 1G and 1H), but not *Sema3a*$^{-/-}$ E9.5 embryos (Figure 1L and 1M), was stereotypically reshaped into a pattern wherein cephalic veins were discernible. Moreover, in E9.5 wild-type (Figure 1D) and *Sema3f*-null (Figure 1I) but not *Sema3a*-null (Figure 1N) embryos, the dorsal longitudinal anastomotical vessel started to be remodeled into a mature perineural capillary plexus.

Sema3F Drives Extraembryonic Angiogenesis

In quest of explanations for the growth retardation associated with an essentially normal vascular development of *Sema3f*-knockout embryos, we reasoned that it may be due to defective angiogenesis in extraembryonic organs, namely, yolk sac and placenta. Accordingly, we observed that, although yolk sacs of E10.5 wild-type embryos contained a dense hierarchically ordered vascular network (Figure 1P, 1Q, 1V, and 1W), *Sema3f*-null yolk sacs unexpectedly displayed a dramatic reduction in blood vessel number and organization into a mature vascular tree (Figure 1R, 1S, 1X, and 1Y). *Sema3f*$^{-/-}$ mice placentas were also highly anemic and abnormally vascularized (Results section; Discussion section, and Figure II in the online-only

Table 2. Number of Intersomitic Vessels Evaluated in *Sema3f*, *Sema3a*, and *Sema3a/Sema3f*-Knockout Embryos (E9.5)

Genotype	Intersomitic Vessels	Genotype	Intersomitic Vessels	Genotype	Intersomitic Vessels
Sema3f$^{+/+}$	21.2±0.5	*Sema3a*$^{+/+}$	21.7±0.6	*Sema3a*$^{+/+}$ *Sema3f*$^{+/+}$	21.0±1.2
Sema3f$^{-/-}$	18.8±0.5	*Sema3a*$^{-/-}$	17.0±1.2	*Sema3a*$^{-/-}$ *Sema3f*$^{-/-}$	11.0±0.6
P=0.0062 (n=6)		*P*=0.0039 (n=7)		*P*=0.0015 (n=3)	

All data are expressed as mean±SEM. *Sema3* indicates class 3 semaphorin.

Data Supplement). A not remodeled primary vascular plexus and occasional scattered blood islands were instead present in *Sema3a*-null yolk sacs (Figure 1T, 1U, 1Z, and 1AA).

The mouse yolk sac consists of mesoderm-derived blood islands and vessels that are positioned between endoderm-derived visceral yolk sac (VYS) epithelial cell (EpC) layer and parietal yolk sac (PYS) EpC layer.[20] VYS EpCs control nutrient and gas exchanges and the development of blood islands and vessels; PYS EpCs instead protect the embryo.[20] To understand which cell types synthesize Sema3F and express the major Sema3F coreceptor Nrp2, we performed confocal microscopy analyses on E9.5 yolk sacs that were double stained with either anti-Sema3F or anti-Nrp2 and antibodies recognizing vascular EnC or VYS EpC or PYS EpC markers, respectively, represented by endomucin, cytokeratin 8/18 (CK8/18), and Snail1 proteins.[21] Sema3F protein was present in VYS EpCs and in part also in vascular EnCs of *Sema3f*$^{+/+}$ but not in *Sema3f*$^{-/-}$ yolk sacs (Figure 2A and 2C). PYS EpCs essentially do not produce Sema3F (Figure 2A and 2C). We next analyzed the expression of Sema3F in E9.5 embryos. As illustrated in Figure IIIC and IIID in the online-only Data Supplement, Sema3F was mainly expressed in vascular EnCs of both wild-type and *Sema3a*$^{-/-}$, but not in *Sema3f*$^{-/-}$, embryos. Similarly, Sema3A was expressed in endomucin^{+} vessels of *Sema3f*$^{-/-}$ yolk sacks (Figure IIIA and IIIB in the online-only Data Supplement).

We also observed that Nrp2, the major Sema3F coreceptor, is expressed in VYS EpCs and vascular EnCs but not in PYS EpCs (Figure 2B and 2D). Thus, in the yolk sac, Nrp2-expressing EnCs and VYS EpCs may be stimulated by paracrine/autocrine Sema3F.

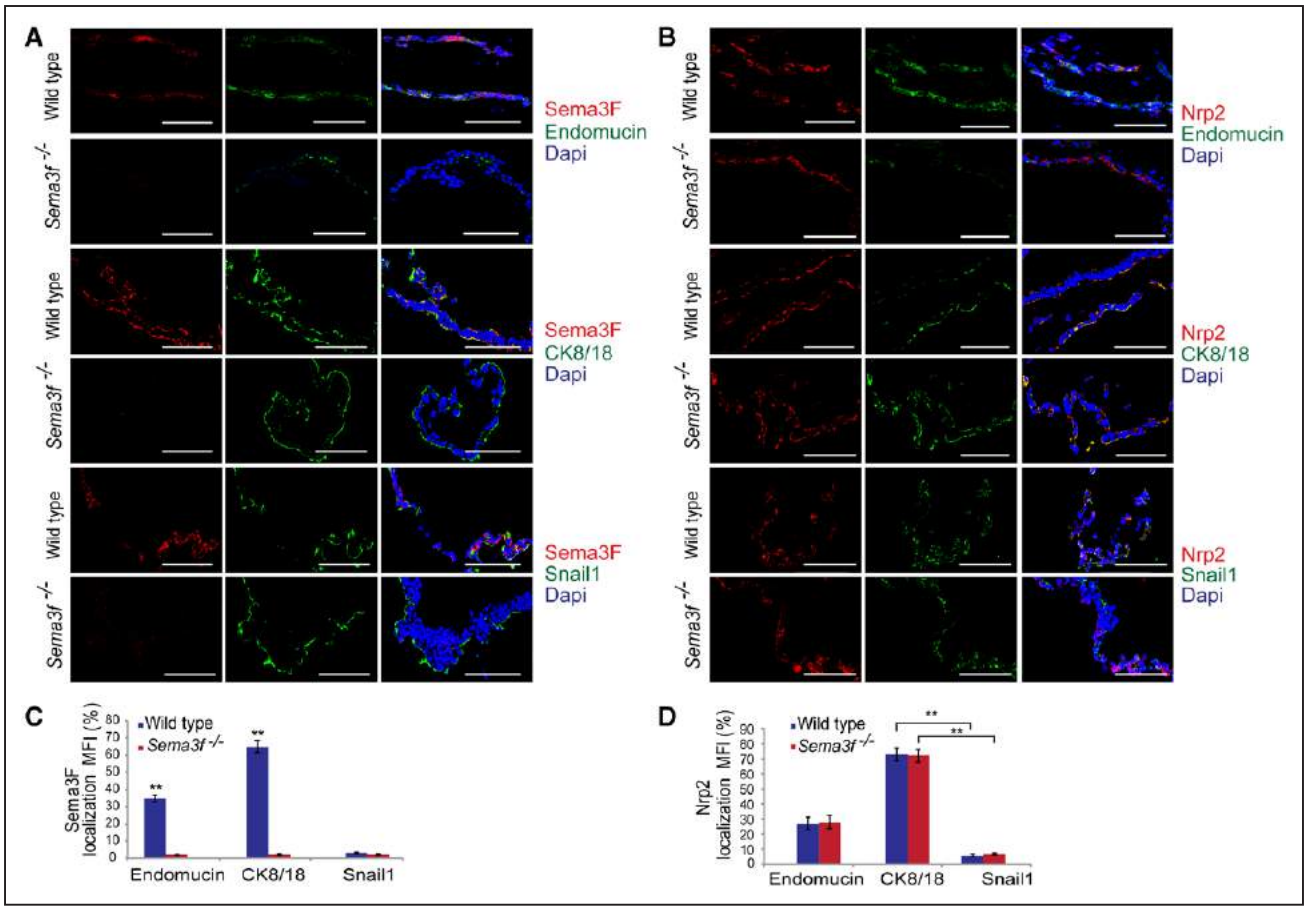

Figure 2. Sema3 (class 3 semaphorin)-F and Nrp2 are mainly expressed by the CK8/18 (cytokeratin 8/18)$^{+}$ epithelial cells of the yolk sac. Frozen sections of yolk sacs were decorated for Sema3F (red) in costaining alternatively with endomucin, CK8/18, or Snail1 antibodies (green) and Dapi (4′,6-diamidino-2-phenylindole; blue). **A**, Sema3F largely colocalized with the CK8/18 visceral epithelial cells marker. As expected, no Sema3F expression was detected in *Sema3f*$^{-/-}$ samples. **B**, Confocal analysis showed that in both *Sema3f*$^{+/+}$ and *Sema3f*$^{-/-}$ mice, Nrp2 is greater expressed by the visceral yolk sac as assessed by Nrp2-CK8/18 costaining. Confocal analysis was performed on tissue sections from 6 mice per group; scale bars, 100 μm. **C** and **D**, Graphs show the percentage of Sema3F and Nrp2 colocalization with endomucin, CK8/18, and Snail1 in both *Sema3f*$^{+/+}$ and *Sema3f*$^{-/-}$ yolk sacs (**P<0.01, Student t test).

Sema3F Signaling Inhibits the Degradation of Myc Transcription Factor in Visceral Yolk Sac Epithelial Cells

Our data indicate that, at odds with its well-characterized antiangiogenic effects reported in the adult animal,[13] Sema3F plays a proangiogenic role in extraembryonic tissues. Because it is well documented that in EnCs Sema3F elicits canonical antiangiogenic signals,[22] we considered the option that Sema3F might exert its proangiogenic activity at least in part by controlling gene transcription in extraembryonic tissues, for example, by acting on Nrp2-expressing VYS EpCs. In this regard, the basic helix-loop-helix transcription factor Myc is a well-established regulator of vascular development,[23] and in *Caenorhabditis elegans*, a Myc-like network was found to cooperate with semaphorin signaling in the control of cell migration.[24] Hence, we first assessed whether the loss of *Sema3f* was associated with the modulation of yolk sac Myc protein expression. Confocal immunofluorescence analysis on E9.5 wild-type and *Sema3f*$^{-/-}$ yolk sacs revealed how Myc protein was decreased by 0.73-fold in *Sema3f*-knockout animals (Figure 3A and 3B).

Myc protein stability is regulated by phosphorylation and ubiquitin-dependent degradation. In particular, GSK3 (glycogen synthase kinase 3)-mediated phosphorylation of Myc at Thr58 gives rise to a binding site that is directly recognized by the E3 ubiquitin ligase Fbw7(F-box and WD repeat domain-containing 7), resulting in ubiquitination followed by proteasomal degradation of Myc.[25] Consistent with previous in vitro data,[25] we found that in E9.5 *Sema3f*$^{-/-}$ yolk sacs the reduction in Myc protein amount was associated with a selective increase of Myc Thr58 phosphorylation in VYS EpCs, but neither in PYS EpCs nor in EnCs (Figure 3C and 3D). Altogether, our findings support a model in which in the mouse yolk sac paracrine/autocrine Sema3F signals to inhibit the (GSK3-dependent) phosphorylation on Thr58 and ensuing degradation of the proangiogenic Myc transcription factor in VYS EpCs. Hence, paracrine/autocrine Sema3F signals inhibit the phosphorylation on Thr58 and ensuing degradation of Myc in VYS EpCs.

Sema3F Promotes the Transcription of Myc-Regulated AngiomiRs in the Mouse Yolk Sac

Myc may drive yolk sac blood vessel development downstream of Sema3F signaling by promoting the transcription of different proangiogenic genes.[23,26] In particular, it was

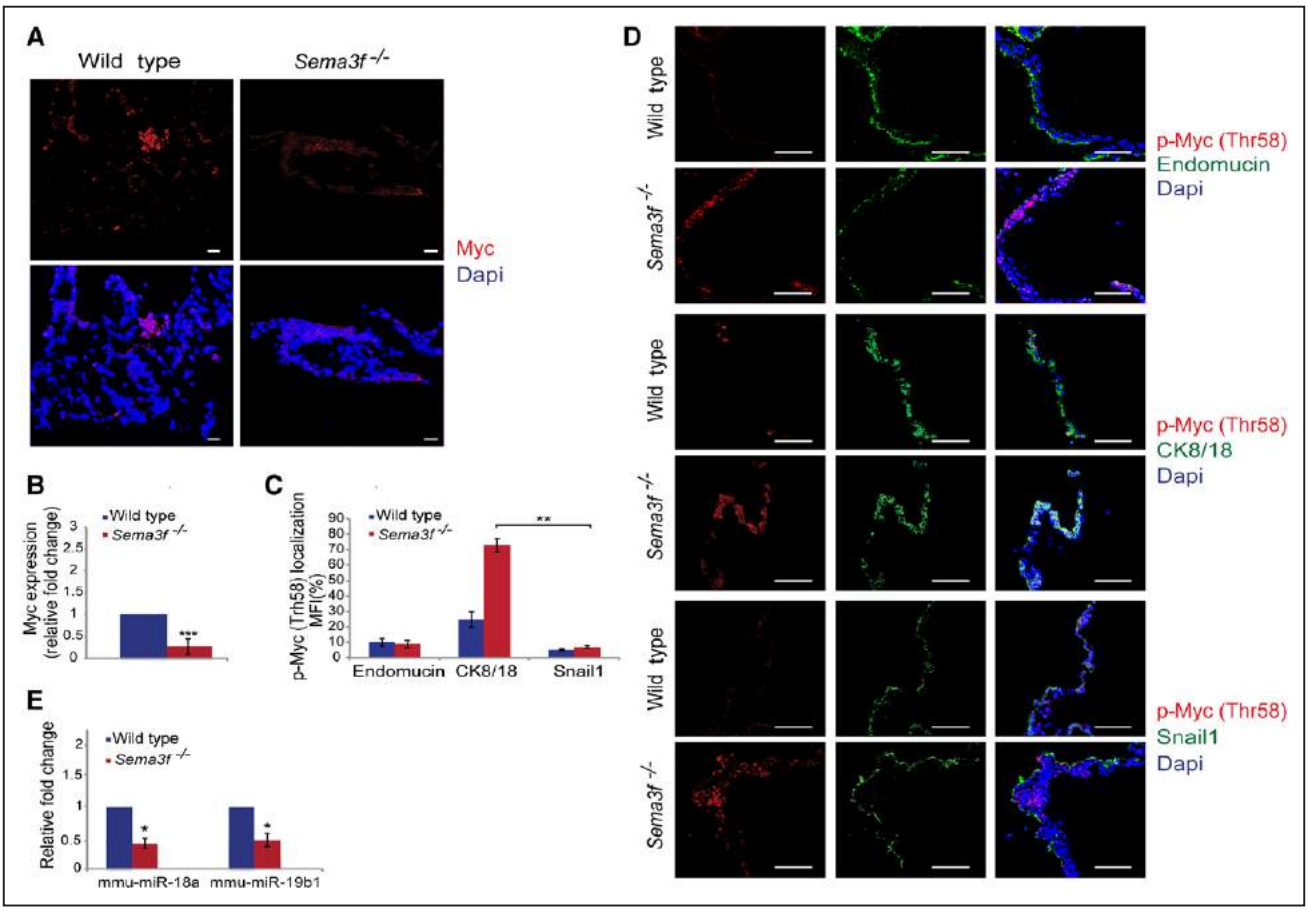

Figure 3. Sema3 (class 3 semaphorin)-F activates a Myc- and miR-18a/miR-19b–dependent proangiogenic pathway in the mouse yolk sac. **A** and **B**, Quantification of immunofluorescence analysis of E9.5 yolk sacs using Myc antibody (red) counterstained with Dapi (4′,6-diamidino-2-phenylindole; blue) showed that Myc expression decreases by 0.73-fold in *Sema3f*$^{-/-}$ yolk sacs. **C** and **D**, Myc phosphorylation at Thr58 significantly increased in E9.5 *Sema3f*$^{-/-}$ yolk sacs compared with the wild type. Furthermore, a double staining with anti-p-Myc (Thr58) and either anti-endomucin or anti–cytokeratin 8/18 (CK8/18), or anti-Snail1 revealed that p-Myc (Thr58) is mainly expressed in CK8/18+ visceral yolk sac epithelial cells, whereas only few amounts of Thbs1 were associated with endomucin^{+} vascular endothelial cells. **E**, Real-time polymerase chain reaction revealed how, compared with wild-type yolk sacs, proangiogenic miR-18a and miR-19b diminished in *Sema3f*$^{-/-}$ yolk sacs. (***P<0.0001; **P<0.01; *P<0.05, Student t test). Scale bars, 100 μm.

reported that in cultured embryonic stem cells, Myc loss impairs *Vegfa* (vascular endothelial growth factor A) gene expression.[23] However, even if Myc protein abundance was dramatically decreased (Figure 3A and 3B), we did not detect any significant reduction of *Vegfa* mRNA in *Sema3f*-null yolk sacs, as evaluated by real-time quantitative polymerase chain reaction (Figure IVA in the online-only Data Supplement). These findings indicate that in the mouse yolk sac, Sema3F should induce the transcription of additional Myc-dependent proangiogenic genes other than *Vegfa*.

Specific miRNA genes, dubbed angiomiRs, are master regulators of developmental angiogenesis and transcription of the key proangiogenic miR-17/92 cluster[26] lies under the control of Myc.[27] Thus, we considered the possibility that Myc protein downmodulation in *Sema3f*$^{-/-}$ yolk sacs may impair miR-17/92 gene cluster transcription. By real-time quantitative polymerase chain reaction, we analyzed the transcription of genes belonging to miR-17/92 cluster in E9.5 wild-type and *Sema3f*$^{-/-}$ yolk sacs. Among miR-17/92 gene cluster members, miR-18a and miR-19b-1 emerged as the most modulated miRNAs in *Sema3f*$^{-/-}$ yolk sacs. Compared with wild type, miR-18a and miR-19b-1 levels, respectively, decreased by 0.5- and 0.8-fold in *Sema3f*$^{-/-}$ yolk sacs (Figure 3E). Hence, Sema3F signaling drives the Myc-mediated transcription of the proangiogenic miR 17/92 cluster members miR-18a and miR-19b-1.

Sema3F Inhibits the Expression of the Antiangiogenic Factor Thbs1 (Thrombospondin 1) in Mouse Visceral Yolk Sac Epithelial Cells

Thbs1 (thrombospondin 1) is an effective angiogenesis inhibitor[28] whose expression is inhibited by Myc protein[23] and Myc-induced miR-17/92 cluster miRNAs,[29] in particular, miR-18a and miR-19b-1.[30–32] To assess whether Thbs1 expression was modulated in E9.5 *Sema3f*$^{-/-}$ yolk sacs compared with their wild-type counterpart, we first analyzed *Thbs1* gene transcription by real-time quantitative polymerase chain reaction (Figure IVB in the online-only Data Supplement). Compared with wild-type yolk sacs, *Thbs1* mRNA levels increased by 1.5-fold in *Sema3f*$^{-/-}$ yolk sacs. Next, we assessed Thbs1 protein expression by confocal immunofluorescence microscopy. Quantitave analysis revealed that, in comparison to wild-type

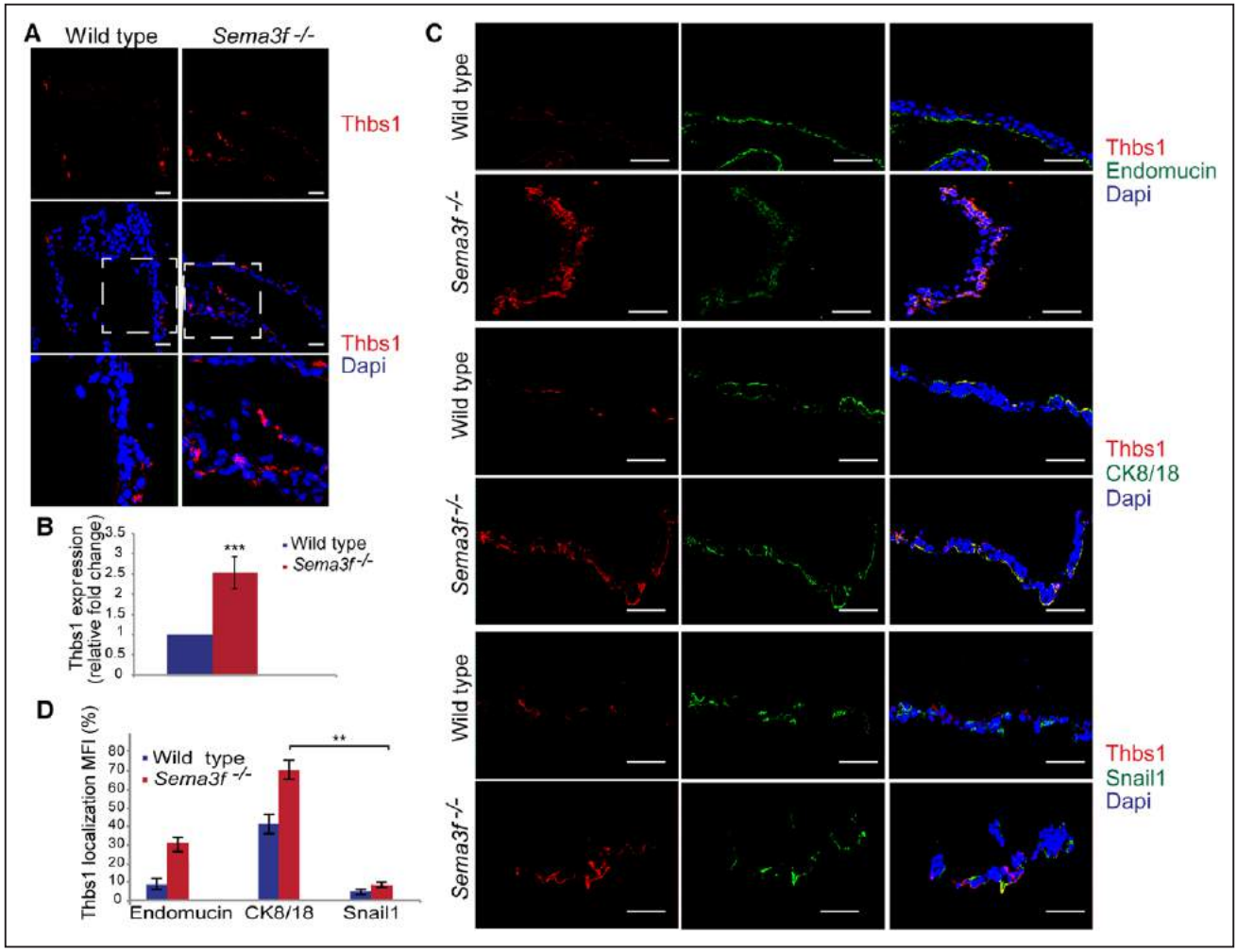

Figure 4. Sema3 (class 3 semaphorin)-F signaling inhibits Thbs1 (thrombospondin 1) protein expression. **A** and **B**, Quantification of immunofluorescence analyses of E9.5 yolk sacs showed that Thbs1 expression increases by 2.5-fold in *Sema3f*$^{-/-}$ yolk sacs. Scale bars, 300 μm (***P*<0.001; ****P*<0.0001, Student *t* test). **C**, Confocal analysis showed that Thbs1 protein expression is enriched in CK8/18 (cytokeratin 8/18)$^{+}$ visceral yolk sac epithelial cells compared with the other cell types. Scale bars, 100 μm. **D**, Bar graph shows the percentage of Thbs1 colocalization with endomucin, CK8/18, and Snail1 in both wild-type and *Sema3f*$^{-/-}$ yolk sacs (***P*<0.001, Student *t* test).

yolk sacs, Thbs1-positive areas increased by 2.5-fold in *Sema3f*$^{-/-}$ yolk sacs (Figure 4A and 4B).

To understand which cell type(s) synthesize Thbs1, we analyzed by confocal microscopy E9.5 yolk sacs that were double stained with anti-Thbs1 and either antiendomucin or anti-CK8/18, or anti-Snail1. We detected Thbs1 protein mainly in CK8/18^{+} VYS EpCs, whereas only a few amount of Thbs1 was associated with endomucin^{+} vascular EnCs (Figure 4C and 4D). Of note, we did not observe any difference in the expression of Thbs2 in the different cell types of *Sema3f*$^{-/-}$, compared with wild-type yolk sacs (Figure V in the online-only Data Supplement).

It has been clearly documented how Thbs1 effectively impairs VEGFA function mostly by inhibiting VEGF-R2 (VEGF receptor 2 phosphorylation).[28,33,34] Therefore, we investigated whether endothelial VEGF signaling may be affected in *Sema3f*-knockout yolk sacs and uncovered that indeed tyrosine phosphorylation VEGF-R2 was reduced dramatically in vascular EnCs of E9.5 *Sema3f*$^{-/-}$ yolk sacs (Figure 5). Hence, in *Sema3f*-null yolk sacs, VYS EpCs synthesize high amount of Thbs1 protein that in turn effectively impairs VEGF-R2 activation in vascular EnCs.

In In Vitro Differentiated VYS EpCs, Exogenous Recombinant Sema3F Inhibits the Myc-Dependent Expression of the Antiangiogenic Factor Thbs1

To directly assess whether Sema3F may stimulate Myc protein accumulation and the decrease of the antiangiogenic factor Thbs1, we set up an in vitro system to create differentiated CK8/18^{+} VYS Eps that may then be treated with recombinant Sema3F (rSema3F). To this aim, we exploited the well-characterized in vitro model of F9 testicular teratocarcinoma stem cells that, when cultured as aggregates in suspension and stimulated with retinoic acid, differentiate in VYS Eps.[35,36] Fluorescent confocal microscopy confirmed that, similar to what observed in the mouse yolk sac (Figure 2B and 2D), in vitro differentiated CK8/18^{+} VYS EpCs expressed Sema3F receptor Nrp2 as well (Figure 6A). Of note, quantitative analysis of immunofluorescent staining revealed how exogenously added rSema3F effectively inhibits the degradative GSK-dependent phosphorylation of Myc on Thr58 (Figure 6B and 6D) and increases total Myc protein levels (Figure 6B and 6D), while significantly decreasing Thbs1 (Figure 6C and 6D), whose expression is known to be inhibited by Myc.[23] Thus, direct in vitro stimulation of cultured VYS Eps with rSema3F promotes the accumulation of Myc and impairs the expression of the antiangiogenic factor Thbs1.

Sema3a Sema3f Double Knockdown Results in Early Mouse Embryonic Lethality and Severely Impairs Both Embryonic and Extraembryonic Angiogenesis

To understand whether Sema3A and Sema3F may cooperate in regulating embryonic development, we first mated *Sema3a*$^{+/-}$ and *Sema3f*$^{+/-}$ mice to create double *Sema3a*$^{+/-}$ *Sema3f*$^{+/-}$ mice that in F1 progeny were born in a normal Mendelian ratio. Then, to generate double *Sema3a/Sema3f*-knockout mice, *Sema3a*$^{+/-}$ *Sema3f*$^{+/-}$ animals were mated. Among 405 weaned mice, no double *Sema3a*$^{-/-}$ *Sema3f*$^{-/-}$ mice were born. These data indicate that all double *Sema3a Sema3f*-knockout mice died in utero. To assess the time of embryo lethality, double *Sema3a*$^{-/-}$ *Sema3f*$^{-/-}$ embryos were genotyped at different gestation times, observing a large loss of double *Sema3a*$^{-/-}$ *Sema3f*$^{-/-}$ embryos around E9.5 (Table 3).

Compared with wild-type animals (Figure 7D), *Sema3a*$^{-/-}$ *Sema3f* $^{-/-}$ embryos were significantly smaller (Figure 7H),

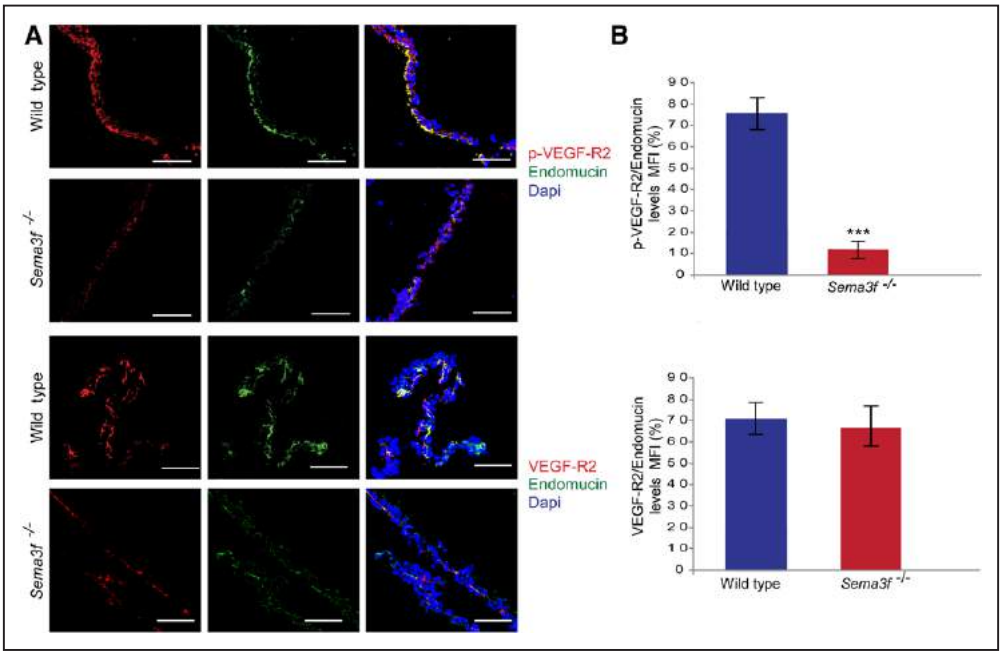

Figure 5. *Sema3f*-knockout impairs VEGF-R2 (vascular endothelial growth factor receptor R2) phosphorylation in the yolk sac. **A**, Confocal microscopy analysis showed that VEGF-R2 phosphorylation is strongly reduced in *Sema3f*$^{-/-}$ yolk sacs compared with wild-type controls, whereas VEGF-R2 expression is not affected. Scale bars, 100 μm. **B**, Percentage of p-VEGF-R2 and total VEGF-R2 relative levels in endomucin^{+} endothelial cell. (***P<0.0001, Student t test). Sema3 indicates class 3 semaphorin.

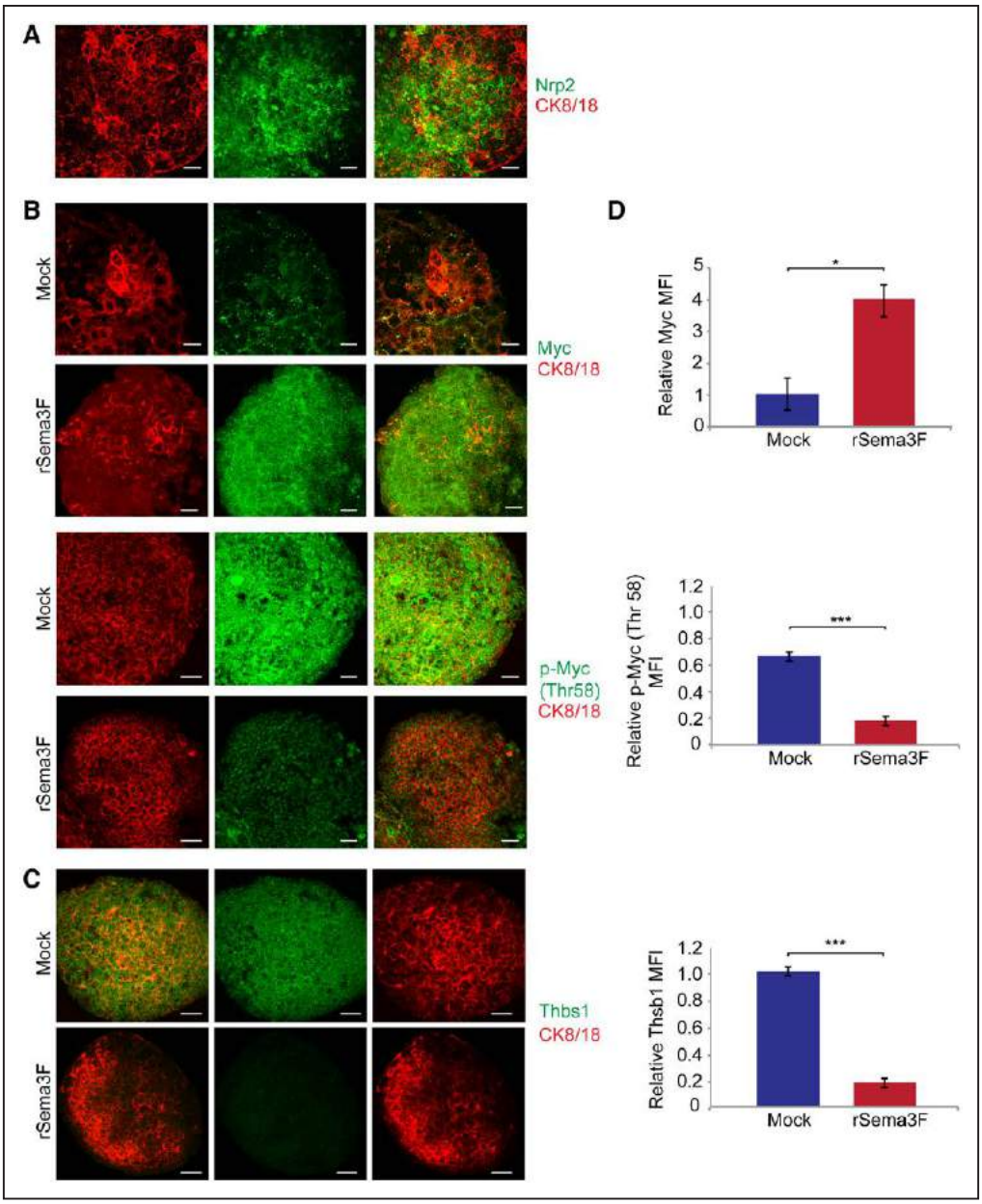

Figure 6. Exogenous recombinant Sema3 (class 3 semaphorin)-F impairs Myc degradation and inhibits Thbs1 (thrombospondin 1) expression in in vitro differentiated visceral yolk sac (VYS) epithelial cells (EpCs). **A**, Mouse F9 teratocarcinoma stem cells differentiated in VYS EpCs express Sema3F receptor Nrp2, as revealed by immunofluorescence staining. **B**, Stimulation with exogenous rSema3F increases Myc expression and reduces Myc Thr58 phosphorylation in in vitro differentiated VYS EpCs derived from mouse F9 teratocarcinoma stem cells. **C**, rSema3F stimulation also decreases the expression of antiangiogenic Thbs1 protein in VYS EpCs derived from mouse F9 teratocarcinoma stem cells. **D**, The relative fluorescence intensity of Myc, Thr58 phosphorylated Myc, and Thbs1 was measured in VYS EpCs derived from mouse F9 teratocarcinoma stem cells stimulated or not with rSema3F. Data are mean±SEM. n=15 cell aggregates per condition pooled from 3 independent experiments. (***P<0.0001; *P<0.05, Student t test). Scale bars, 25 μm.

and their growth delay at E9.5 was more important than that observed in *Sema3a*$^{-/-}$ embryos (Figure 1O). In fact, on average, at E9.5, *Sema3a*$^{-/-}$ *Sema3f*$^{-/-}$ embryos displayed 11 somites compared with the 21 somites of wild-type littermates (Table 2). Confocal immunofluorescence microscopy on whole-mount endomucin-stained *Sema3a*$^{-/-}$ *Sema3f* $^{-/-}$ embryos (Figure 7E through 7G) unveiled how vascular abnormalities were considerably more severe than those observed in *Sema3a*-null mice (Figure 1K through 1N). In particular, compared with wild-type embryos (Figure 7A through 7C), both cephalic vascular plexus (Figure 7E and 7F) and intersomitic blood vessels (Figure 7E and 7G) were poorly formed and, when formed, they were not remodeled. Short noninterconnected sprouts enclosed wide avascular spaces. Next, we evaluated the impact of *Sema3a Sema3f*-double knockout on yolk sac vascularization. Because of the difficulties in recovering viable double *Sema3a*$^{-/-}$ *Sema3f*$^{-/-}$ mutant embryos at E10.5, we decided to analyze the vasculature of E9.5 yolk sacs, which, differently from wild-type yolk sacs (Figure 7I), appeared extremely pale and essentially avascular (Figure 7J).

Table 3. Genotypes of Progeny from *Sema3a*$^{+/-}$/*Sema3f*$^{+/-}$ Intercrosses

	Total	*3a*$^{+/+}$/*3f*$^{+/+}$	*3a*$^{+/-}$/*3f*$^{+/-}$	*3a*$^{+/-}$/*3f*$^{+/+}$	*3a*$^{+/+}$/*3f*$^{+/-}$	*3a*$^{-/-}$/*3f*$^{+/-}$	*3a*$^{+/+}$/*3f*$^{-/-}$	*3a*$^{+/-}$/*3f*$^{-/-}$	*3a*$^{-/-}$/*3f*$^{+/+}$	*3a*$^{-/-}$/*3f*$^{-/-}$
Term Pups	405	10.1% (41)	35.8% (145)	21.4% (87)	17.3% (70)	3.5% (14)	3.5% (14)	4.9% (20)	3.5% (14)	0% (0)
E9.5	387	6.46% (25)	21.44% (83)	11.1% (43)	13.9% (54)	9.8% (38)	5.2% (20)	9.6% (37)	5.6% (22)	3.6% (14)
Expected Mendelian ratio		6.25%	25%	12.5%	12.5%	12.5%	6.25%	12.5%	6.25%	6.25%

Heterozygous *Sema3a*$^{+/-}$/*Sema3f*$^{+/-}$ mice were intercrossed, and the progeny was analyzed. No adult double *Sema3a Sema3f*-knockout mice were observed after genotyping the offspring (n=405). Timed mating revealed an embryonic lethality until E9.5, and only the 3.6% (n=387) were *Sema3a*$^{-/-}$/*Sema3f*$^{-/-}$ at E9.5. This percentage is the half than the Mendelian expected ratio. *Sema3* indicates class 3 semaphorin.

Thus, abnormalities of *Sema3a*$^{-/-}$ *Sema3f*$^{-/-}$ yolk sac blood vessels (Figure 7J) were considerably more serious than those observed in either *Sema3f*$^{-/-}$ (Figure 1R, 1S, 1X, and 1Y) or *Sema3a*$^{-/-}$ (Figure 1T, 1U, 1Z, and 1AA) yolk sacs.

Discussion

The formation of properly patterned intraembryonic and extraembryonic blood vessel networks is crucial to development of vertebrate organisms.[1] By counteracting the activity of proangiogenic factors such as VEGFA, antiangiogenic Sema3 proteins, eg, Sema3A and Sema3E, play key roles in shaping blood vascular patterns of developing embryos.[12] Here, we unveil how, as a notable exception, Sema3F selectively exerts an effective proangiogenic activity during extraembryonic, but not intraembryonic, vascular development. The defective vascularization of *Sema3f*-null yolk sacs phenocopies the defects of *Nrp1*$^{-/-}$ *Nrp2*$^{-/-}$ embryos that have nearly avascular yolk sacs.[37] In addition, we observed that *Sema3f*$^{-/-}$ placentas are also anemic (Results section and Discussion section in the online-only Data Supplement). Sema3F signaling mainly relies on Nrp2 coreceptor.[6] However, in the absence of Nrp2, Sema3F can also signal via Nrp1[38] and dissociation constants for Sema3F binding to Nrp1 and Nrp2 are 1.1 and 0.09 nmol/L, respectively.[39] Altogether, our and previous data suggests that both Nrp1 and Nrp2 may be required to allow Sema3F-promoting extraembryonic vascular development.

In *Sema3f*$^{-/-}$ yolk sacs, we observed a significant downregulation of Myc, a transcription factor that regulates the expression of several gene sets, such as those promoting developmental[23] and tumor[29] angiogenesis. Myc protein levels are regulated by GSK3 that, by phosphorylating Myc on Thr58, generates a phosphodegron that enables Fbw7 ubiquitin ligase binding, Myc ubiquitylation, and proteasomal degradation.[25] Notably, as previously reported in cultured cells,[25] we also found that in *Sema3f*$^{-/-}$ yolk sacs, the drop in Myc protein abundance was combined with an increased Myc Thr58 phosphorylation in Nrp2-expressing VYS EpCs. Fittingly, we also observed that the treatment of in vitro differentiated Nrp2^{+} VYS EpCs with exogenous Sema3F decreases Myc Thr58 phosphorylation, thus promoting Myc accumulation. In EnCs, Sema3F inhibits the phosphatidylinositol 3 kinase-dependent activation of Akt[22] that is known to phosphorylate and inactivate GSK3.[40] It seems that instead in VYS EpCs autocrine/paracrine Sema3F, by either activating a GSK3 kinase (such as Akt, p90RSK, p70S6K, and PKA) or inhibiting a GSK3-phosphatase (eg, PP2A), impairs the GSK3-dependent phosphorylation of Myc on Thr58 and its ensuing degradation. Further work is needed to establish the diverse molecular mechanisms by which Sema3F may activate or inhibit GSK3 function in different cell types.

MiRNAs are central regulators of cardiovascular development, and Myc promotes the transcription of the miR-17/92 cluster,[26,27] whose members miR-18a and miR-19b-1 target the angiogenesis inhibitor Thbs1 hence promoting blood vessel formation.[30,31] We revealed how lack of Sema3F results in reduced miR-18a and miR-19b-1 gene transcription, increased Thbs1 protein in VYS EpCs, and dramatically reduced VEGF-R2 tyrosine phosphorylation in vascular EnCs of E9.5 *Sema3f*$^{-/-}$ yolk sacs. Consistently, we also observed that exogenous Sema3F strongly inhibits the expression of Thbs1 protein in in vitro differentiated Nrp2^{+} VYS EpCs.

Our findings unveil a reciprocal cellular cross-talk that supports extraembryonic angiogenesis in the yolk sac (depicted in Figure VI in the online-only Data Supplement). In VYS EpCs, Sema3F, which is produced by both VYS EpCs and EnCs, signals to counteract the GSK3-driven degradative phosphorylation of Myc on Thr58, thus fostering the Myc-dependent transcription of proangiogenic miR-17/92 cluster members that in turn inhibit the synthesis of the antiangiogenic protein Thbs1 in VYS EpCs themselves, finally allowing EnCs to be elicited by VEGFA, which is also secreted by VYS EpCs and required for yolk sac vascularization.[41] In sum, we provide evidence that the extraembryonic proangiogenic activity of Sema3F relies on the Myc-dependent inhibition of the antiangiogenic protein Thbs1, which in turn is an effective inhibitor of VEGF signaling.[33] Indeed, the Thbs1 receptor CD36 has been shown to physically interact with VEGF-R2 and hamper its ligand-induced phosphorylation and biological activity on EnCs.[28,33] Mechanistically, it was reported that Thbs1 binding to CD36 recruits the SHP-1(Src homology 2 domain–containing protein tyrosine phosphatase-1) to the CD36–VEGF-R2 complex, where SHP-1 dephosphorylates and inactivates VEGF-R2 proangiogenic signaling.[34]

In light of the fact that another Nrp2-binding semaphorin, that is, SEMA3B, was already suggested to be involved in human preeclampsia,[42] our finding that *Sema3f* knockdown severely impairs placentas development and vascularization suggests that an abnormal expression of Sema3F might be implicated in placenta vascular malformations and malignant tumors (Results section, Discussion section, and Figure II in the online-only Data Supplement).

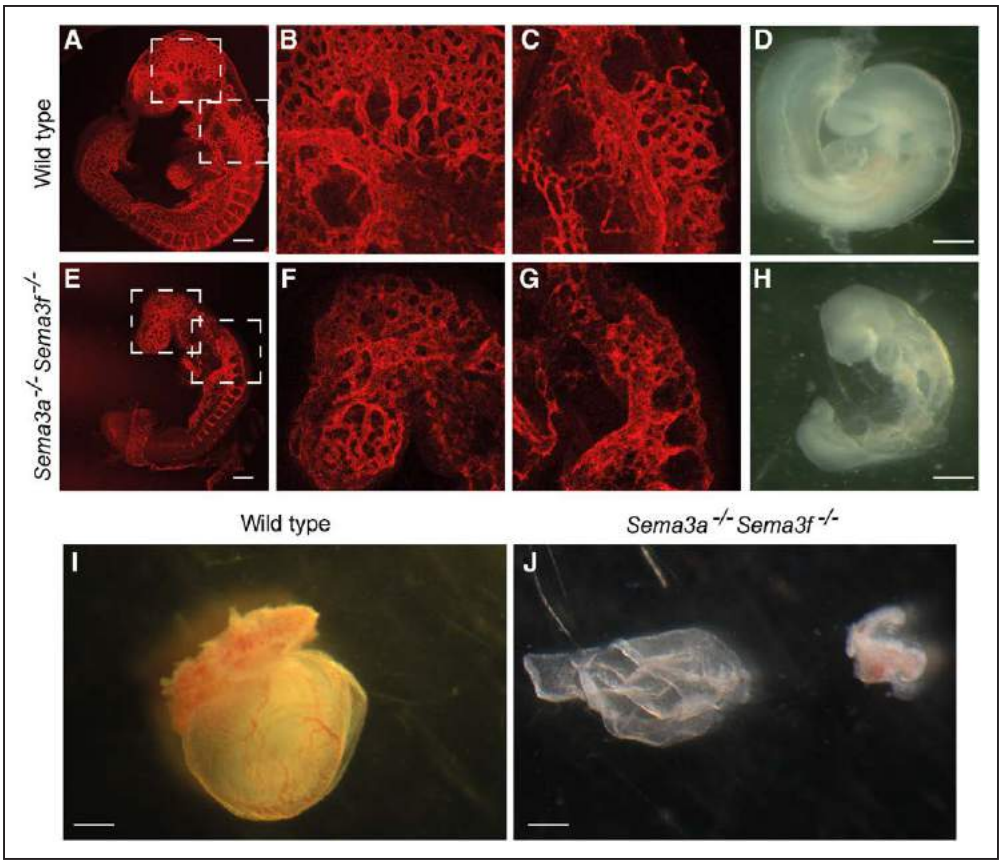

Figure 7. Sema3 (class 3 semaphorin)-F and Sema3A cooperate to control developmental angiogenesis. Whole-mount endomucin-stained E9.5 wild-type (**A**, **B**, and **C**) and *Sema3a*$^{-/-}$ *Sema3f*$^{-/-}$-double knockout (**E**, **F**, and **G**) embryos. Remodeling of the cephalic plexus into veins occurs in wild type (**A** and **B**) but not in *Sema3a*$^{-/-}$ *Sema3f*$^{-/-}$ (**E** and **F**) embryos. Similarly, the dorsal longitudinal anastomotical vessel is remodeled in the cephalic perineural vascular plexus in wild type (**A** and **C**) but not in *Sema3a*$^{-/-}$ *Sema3f*$^{-/-}$ (**E** and **G**) embryos. Stereomicroscopic analyses revealed how, when compared with age-matched wild-type embryos (**D**), the development of *Sema3a*$^{-/-}$ *Sema3f*$^{-/-}$ (**H**) E9.5 embryos is severely delayed. Stereomicroscopy analysis (**I** and **J**) of E10.5 wild-type (**I**) and *Sema3a*$^{-/-}$ *Sema3f*$^{-/-}$ (**J**) yolk sacs. *Sema3a*$^{-/-}$ *Sema3f*$^{-/-}$ yolk sacs (**J**) are essentially avascular. **B** and **F**, Magnifications of the top boxed areas in (**A**) and (**E**), respectively. (**C**) and (**G**) are magnifications of bottom boxed areas in (**A**) and (**E**), respectively. Scale bars, 300 μm (**A** and **E**) and 100 μm (**D**, **H**, **I**, and **J**).

As previously reported in zebrafish,[9] chick,[10] and mouse embryos,[8,17–19] here we further substantiate how, differently from Sema3F, Sema3A is a crucial driver of embryonic vascular morphogenesis. Our findings that ≈80% of *Sema3a*-knockout embryos die in utero and display a strong growth retardation compared with wild-type embryos reconcile previous apparently contradicting observations that, based on age and stage matching between wild-type and *Sema3a*-null embryos, concluded that Sema3A does not influence embryonic angiogenesis.[43] Furthermore, we establish how Sema3A similarly controls the remodeling of the yolk sac vasculature.

We found that in *Sema3a*-knockout mice, embryonic and extraembryonic blood vessels develop but display severe defects remodeling into an optimized hierarchically branched mature vascular tree. On the contrary, in *Sema3f*-knockout mice, embryonic blood vessels are effectively remodeled into a mature and functional tree, whereas vascularization of extraembryonic tissues is strongly reduced and poorly branched. It seems that, compared with *Sema3f*$^{-/-}$ yolk sacs, the simultaneous knockdown of *Sema3a* and *Sema3f* gene further impairs the vascularization of the yolk sac that, until E12.5, is the primary means of nutrient, gas, and waste exchange for the mouse embryo.[3] Therefore, our findings suggest that the further dramatic impairment of embryonic vascular remodeling observed in *Sema3a/Sema3f*-double knockout embryos, compared with *Sema3a*$^{-/-}$ embryos, is conceivably because of the severe disruption of the vasculature of the yolk sac, which constitutes the main nutrient and gas exchange organ between mother and embryo. Our data are in agreement with the fact that the yolk sac constitutes the first main nutrient and gas exchange organ between mother and embryo and with previous observations that mutations causing severe disruption yolk sac blood vessel formation are lethal and result in severe defects in embryo development.[44–51] Finally, the severe disruption of the embryonic vasculature observed in *Sema3a/Sema3f*-double knockout phenocopy the previously described vascular phenotype of double targeted *Nrp1*$^{-/-}$ *Nrp2*$^{-/-}$ embryos.[37]

Acknowledgments

E. Giraudo, and G. Serini conceived the project; E. Giraudo, G. Serini, F. Bussolino, and F. Maione designed the experiments; D. Regano, F. Maione, A. Visintin, F. Clapero, and D. Valdembri performed the experiments; E. Giraudo, G. Serini, D. Regano, F. Maione, A. Visintin, F. Clapero, and D. Valdembri analyzed the data;

E. Giraudo, G. Serini, D. Regano, F. Maione, A. Visintin, F. Clapero, and D. Valdembri interpreted the results; D. Regano, F. Maione, F. Clapero, D. Valdembri, G. Serini, and E. Giraudo wrote the paper; and all authors read and approved the article.

Sources of Funding

This work was supported by grants from Italian Association for Cancer Research (AIRC-IG grant number: 15645 to E. Giraudo; grant numbers 13016 and 16702 to G. Serini; grant number 10133 to F. Bussolino; and AIRC 5x1000 grant number 12182 to F. Bussolino); FPRC-ONLUS grant MIUR 2010 Vaschetto - 5 per mille 2010 MIUR (to E. Giraudo and G. Serini); FPRC 5xmille 2014 Ministero Salute (to E. Giraudo and G. Serini); Swiss National Science Foundation, Sinergia grant (number CRSII3 160742/1 to E. Giraudo); Fondi di Ricerca Locale (ex 60% 2015, 2016), University of Turin (to E. Giraudo and G. Serini); Fondo Investimenti per la Ricerca di Base RBAP11BYNP (Newton to F. Bussolino); European Community-FP7, contract 318035 (Biloba to F. Bussolino). Telethon Italy (GGP09175 to G. Serini); and Associazione Augusto per la Vita (to G. Serini). D. Regano was supported by FPRC-ONLUS grant MIUR 2010 Vaschetto-Chiodo Fellowship; and F. Maione was supported by postdoctoral fellowships 2014 granted by Fondazione Umberto Veronesi.

Disclosures

None.

References

1. Herbert SP, Stainier DY. Molecular control of endothelial cell behaviour during blood vessel morphogenesis. *Nat Rev Mol Cell Biol*. 2011;12:551–564. doi: 10.1038/nrm3176.
2. Hirschi KK. Hemogenic endothelium during development and beyond. *Blood*. 2012;119:4823–4827. doi: 10.1182/blood-2011-12-353466.
3. Watson ED, Cross JC. Development of structures and transport functions in the mouse placenta. *Physiology (Bethesda)*. 2005;20:180–193.
4. Hahn C, Schwartz MA. Mechanotransduction in vascular physiology and atherogenesis. *Nat Rev Mol Cell Biol*. 2009;10:53–62. doi: 10.1038/nrm2596.
5. Worzfeld T, Swiercz JM, Sentürk A, Genz B, Korostylev A, Deng S, Xia J, Hoshino M, Epstein JA, Chan AM, Vollmar B, Acker-Palmer A, Kuner R, Offermanns S. Genetic dissection of plexin signaling in vivo. *Proc Natl Acad Sci USA*. 2014;111:2194–2199. doi: 10.1073/pnas.1308418111.
6. Worzfeld T, Offermanns S. Semaphorins and plexins as therapeutic targets. *Nat Rev Drug Discov*. 2014;13:603–621. doi: 10.1038/nrd4337.
7. Serini G, Napione L, Bussolino F. Integrins team up with tyrosine kinase receptors and plexins to control angiogenesis. *Curr Opin Hematol*. 2008;15:235–242. doi: 10.1097/MOH.0b013e3282fa745b.
8. Serini G, Valdembri D, Zanivan S, Morterra G, Burkhardt C, Caccavari F, Zammataro L, Primo L, Tamagnone L, Logan M, Tessier-Lavigne M, Taniguchi M, Püschel AW, Bussolino F. Class 3 semaphorins control vascular morphogenesis by inhibiting integrin function. *Nature*. 2003;424:391–397. doi: 10.1038/nature01784.
9. Torres-Vázquez J, Gitler AD, Fraser SD, Berk JD, Pham VN, Fishman MC, Childs S, Epstein JA, Weinstein BM. Semaphorin-plexin signaling guides patterning of the developing vasculature. *Dev Cell*. 2004;7:117–123. doi: 10.1016/j.devcel.2004.06.008.
10. Bates D, Taylor GI, Minichiello J, Farlie P, Cichowitz A, Watson N, Klagsbrun M, Mamluk R, Newgreen DF. Neurovascular congruence results from a shared patterning mechanism that utilizes semaphorin3A and neuropilin-1. *Dev Biol*. 2003;255:77–98.
11. Gu C, Yoshida Y, Livet J, Reimert DV, Mann F, Merte J, Henderson CE, Jessell TM, Kolodkin AL, Ginty DD. Semaphorin 3E and plexin-D1 control vascular pattern independently of neuropilins. *Science*. 2005;307:265–268. doi: 10.1126/science.1105416.
12. Wälchli T, Wacker A, Frei K, Regli L, Schwab ME, Hoerstrup SP, Gerhardt H, Engelhardt B. Wiring the vascular network with neural cues: a CNS perspective. *Neuron*. 2015;87:271–296. doi: 10.1016/j.neuron.2015.06.038.
13. Tamagnone L. Emerging role of semaphorins as major regulatory signals and potential therapeutic targets in cancer. *Cancer Cell*. 2012;22:145–152. doi: 10.1016/j.ccr.2012.06.031.
14. Serini G, Bussolino F, Maione F, Giraudo E. Class 3 semaphorins: physiological vascular normalizing agents for anti-cancer therapy. *J Intern Med*. 2013;273:138–155. doi: 10.1111/joim.12017.
15. Walz A, Feinstein P, Khan M, Mombaerts P. Axonal wiring of guanylate cyclase-D-expressing olfactory neurons is dependent on neuropilin 2 and semaphorin 3F. *Development*. 2007;134:4063–4072. doi: 10.1242/dev.008722.
16. Taniguchi M, Yuasa S, Fujisawa H, Naruse I, Saga S, Mishina M, Yagi T. Disruption of semaphorin III/D gene causes severe abnormality in peripheral nerve projection. *Neuron*. 1997;19:519–530.
17. Reidy KJ, Villegas G, Teichman J, Veron D, Shen W, Jimenez J, Thomas D, Tufro A. Semaphorin3a regulates endothelial cell number and podocyte differentiation during glomerular development. *Development*. 2009;136:3979–3989. doi: 10.1242/dev.037267.
18. Joza S, Wang J, Tseu I, Ackerley C, Post M. Fetal, but not postnatal, deletion of semaphorin-neuropilin-1 signaling affects murine alveolar development. *Am J Respir Cell Mol Biol*. 2013;49:627–636. doi: 10.1165/rcmb.2012-0407OC.
19. Joza S, Wang J, Fox E, Hillman V, Ackerley C, Post M. Loss of semaphorin-neuropilin-1 signaling causes dysmorphic vascularization reminiscent of alveolar capillary dysplasia. *Am J Pathol*. 2012;181:2003–2017. doi: 10.1016/j.ajpath.2012.08.037.
20. Bielinska M, Narita N, Wilson DB. Distinct roles for visceral endoderm during embryonic mouse development. *Int J Dev Biol*. 1999;43:183–205.
21. Yagi S, Tagawa Y, Shiojiri N. Transdifferentiation of mouse visceral yolk sac cells into parietal yolk sac cells *in vitro*. *Biochem Biophys Res Commun*. 2016;470:917–923. doi: 10.1016/j.bbrc.2016.01.149.
22. Nakayama H, Bruneau S, Kochupurakkal N, Coma S, Briscoe DM, Klagsbrun M. Regulation of mTOR signaling by semaphorin 3F-neuropilin 2 interactions in vitro and in vivo. *Sci Rep*. 2015;5:11789. doi: 10.1038/srep11789.
23. Baudino TA, McKay C, Pendeville-Samain H, Nilsson JA, Maclean KH, White EL, Davis AC, Ihle JN, Cleveland JL. c-Myc is essential for vasculogenesis and angiogenesis during development and tumor progression. *Genes Dev*. 2002;16:2530–2543. doi: 10.1101/gad.1024602.
24. Pickett CL, Breen KT, Ayer DE. A C. elegans Myc-like network cooperates with semaphorin and Wnt signaling pathways to control cell migration. *Dev Biol*. 2007;310:226–239. doi: 10.1016/j.ydbio.2007.07.034.
25. Liu L, Eisenman RN. Regulation of c-Myc protein abundance by a protein phosphatase 2A-glycogen synthase kinase 3β-negative feedback pathway. *Genes Cancer*. 2012;3:23–36. doi: 10.1177/1947601912448067.
26. Doebele C, Bonauer A, Fischer A, Scholz A, Reiss Y, Urbich C, Hofmann WK, Zeiher AM, Dimmeler S. Members of the microRNA-17-92 cluster exhibit a cell-intrinsic antiangiogenic function in endothelial cells. *Blood*. 2010;115:4944–4950. doi: 10.1182/blood-2010-01-264812.
27. Bui TV, Mendell JT. Myc: maestro of microRNAs. *Genes Cancer*. 2010;1:568–575. doi: 10.1177/1947601910377491.
28. Lawler PR, Lawler J. Molecular basis for the regulation of angiogenesis by thrombospondin-1 and -2. *Cold Spring Harb Perspect Med*. 2012;2:a006627. doi: 10.1101/cshperspect.a006627.
29. Dews M, Homayouni A, Yu D, Murphy D, Sevignani C, Wentzel E, Furth EE, Lee WM, Enders GH, Mendell JT, Thomas-Tikhonenko A. Augmentation of tumor angiogenesis by a Myc-activated microRNA cluster. *Nat Genet*. 2006;38:1060–1065. doi: 10.1038/ng1855.
30. Suárez Y, Fernández-Hernando C, Yu J, Gerber SA, Harrison KD, Pober JS, Iruela-Arispe ML, Merkenschlager M, Sessa WC. Dicer-dependent endothelial microRNAs are necessary for postnatal angiogenesis. *Proc Natl Acad Sci USA*. 2008;105:14082–14087. doi: 10.1073/pnas.0804597105.
31. Ohgawara T, Kubota S, Kawaki H, Kondo S, Eguchi T, Kurio N, Aoyama E, Sasaki A, Takigawa M. Regulation of chondrocytic phenotype by micro RNA 18a: involvement of Ccn2/Ctgf as a major target gene. *FEBS Lett*. 2009;583:1006–1010. doi: 10.1016/j.febslet.2009.02.025.
32. Zhu X, Yang Y, Han T, Yin G, Gao P, Ni Y, Su X, Liu Y, Yao Y. Suppression of microRNA-18a expression inhibits invasion and promotes apoptosis of human trophoblast cells by targeting the estrogen receptor α gene. *Mol Med Rep*. 2015;12:2701–2706. doi: 10.3892/mmr.2015.3724.
33. Zhang X, Kazerounian S, Duquette M, Perruzzi C, Nagy JA, Dvorak HF, Parangi S, Lawler J. Thrombospondin-1 modulates vascular endothelial growth factor activity at the receptor level. *FASEB J*. 2009;23:3368–3376. doi: 10.1096/fj.09-131649.
34. Chu LY, Ramakrishnan DP, Silverstein RL. Thrombospondin-1 modulates VEGF signaling via CD36 by recruiting SHP-1 to VEGFR2 complex in microvascular endothelial cells. *Blood*. 2013;122:1822–1832. doi: 10.1182/blood-2013-01-482315.

35. Hogan BL, Taylor A, Adamson E. Cell interactions modulate embryonal carcinoma cell differentiation into parietal or visceral endoderm. *Nature*. 1981;291:235–237.
36. Thompson JR, Gudas LJ. Retinoic acid induces parietal endoderm but not primitive endoderm and visceral endoderm differentiation in F9 teratocarcinoma stem cells with a targeted deletion of the Rex-1 (Zfp-42) gene. *Mol Cell Endocrinol*. 2002;195:119–133.
37. Takashima S, Kitakaze M, Asakura M, Asanuma H, Sanada S, Tashiro F, Niwa H, Miyazaki Ji J, Hirota S, Kitamura Y, Kitsukawa T, Fujisawa H, Klagsbrun M, Hori M. Targeting of both mouse neuropilin-1 and neuropilin-2 genes severely impairs developmental yolk sac and embryonic angiogenesis. *Proc Natl Acad Sci USA*. 2002;99:3657–3662. doi: 10.1073/pnas.022017899.
38. Nasarre P, Constantin B, Rouhaud L, Harnois T, Raymond G, Drabkin HA, Bourmeyster N, Roche J. Semaphorin SEMA3F and VEGF have opposing effects on cell attachment and spreading. *Neoplasia*. 2003;5:83–92.
39. Chen H, Chédotal A, He Z, Goodman CS, Tessier-Lavigne M. Neuropilin-2, a novel member of the neuropilin family, is a high affinity receptor for the semaphorins Sema E and Sema IV but not Sema III. *Neuron*. 1997;19:547–559.
40. Wong KK, Engelman JA, Cantley LC. Targeting the PI3K signaling pathway in cancer. *Curr Opin Genet Dev*. 2010;20:87–90. doi: 10.1016/j.gde.2009.11.002.
41. Damert A, Miquerol L, Gertsenstein M, Risau W, Nagy A. Insufficient VEGFA activity in yolk sac endoderm compromises haematopoietic and endothelial differentiation. *Development*. 2002;129:1881–1892.
42. Zhou Y, Gormley MJ, Hunkapiller NM, Kapidzic M, Stolyarov Y, Feng V, Nishida M, Drake PM, Bianco K, Wang F, McMaster MT, Fisher SJ. Reversal of gene dysregulation in cultured cytotrophoblasts reveals possible causes of preeclampsia. *J Clin Invest*. 2013;123:2862–2872. doi: 10.1172/JCI66966.
43. Vieira JM, Schwarz Q, Ruhrberg C. Selective requirements for NRP1 ligands during neurovascular patterning. *Development*. 2007;134:1833–1843. doi: 10.1242/dev.002402.
44. Millauer B, Wizigmann-Voos S, Schnürch H, Martinez R, Møller NP, Risau W, Ullrich A. High affinity VEGF binding and developmental expression suggest Flk-1 as a major regulator of vasculogenesis and angiogenesis. *Cell*. 1993;72:835–846.
45. Dickson MC, Martin JS, Cousins FM, Kulkarni AB, Karlsson S, Akhurst RJ. Defective haematopoiesis and vasculogenesis in transforming growth factor-beta 1 knock out mice. *Development*. 1995;121:1845–1854.
46. Fong GH, Rossant J, Gertsenstein M, Breitman ML. Role of the Flt-1 receptor tyrosine kinase in regulating the assembly of vascular endothelium. *Nature*. 1995;376:66–70. doi: 10.1038/376066a0.
47. Healy AM, Rayburn HB, Rosenberg RD, Weiler H. Absence of the blood-clotting regulator thrombomodulin causes embryonic lethality in mice before development of a functional cardiovascular system. *Proc Natl Acad Sci USA*. 1995;92:850–854.
48. Mustonen T, Alitalo K. Endothelial receptor tyrosine kinases involved in angiogenesis. *J Cell Biol*. 1995;129:895–898.
49. Winnier G, Blessing M, Labosky PA, Hogan BL. Bone morphogenetic protein-4 is required for mesoderm formation and patterning in the mouse. *Genes Dev*. 1995;9:2105–2116.
50. Boucher DM, Pedersen RA. Induction and differentiation of extra-embryonic mesoderm in the mouse. *Reprod Fertil Dev*. 1996;8:765–777.
51. Carmeliet P, Ferreira V, Breier G, et al. Abnormal blood vessel development and lethality in embryos lacking a single VEGF allele. *Nature*. 1996;380:435–439. doi: 10.1038/380435a0.

Highlights

- Sema3 (class 3 semaphorin)-F is a novel extraembryonic proangiogenic factor.
- Sema3F inhibits the degradative phosphorylation of Myc on Thr58 in visceral yolk sac epithelial cells, both in vivo and in vitro.
- In the mouse yolk sac, Sema3F fosters the transcription of members of the Myc-dependent proangiogenic miR-17/92 cluster.
- Sema3F inhibits the synthesis of the Myc target and antiangiogenic protein thrombospondin 1 in visceral yolk sac epithelial cells, both in vivo and in vitro.
- Sema3F promotes the phosphorylation of vascular endothelial growth factor receptor 2 in yolk sac vascular endothelial cells.

Arteriosclerosis, Thrombosis, and Vascular Biology

JOURNAL OF THE AMERICAN HEART ASSOCIATION

Sema3F (Semaphorin 3F) Selectively Drives an Extraembryonic Proangiogenic Program

Donatella Regano, Alessia Visintin, Fabiana Clapero, Federico Bussolino, Donatella Valdembri, Federica Maione, Guido Serini and Enrico Giraudo

Arterioscler Thromb Vasc Biol. 2017;37:1710-1721; originally published online July 20, 2017;
doi: 10.1161/ATVBAHA.117.308226
Arteriosclerosis, Thrombosis, and Vascular Biology is published by the American Heart Association, 7272 Greenville Avenue, Dallas, TX 75231

Print ISSN: 1079-5642. Online ISSN: 1524-4636

Materials and Methods

Animals

C57Bl/6 mice carrying the *Sema3a*-null allele[1] or C57Bl/6;129P2/OlaHsd carrying the *Sema3f*-null allele [2] were previously described and respectively obtained from the RIKEN BioResource Center (strain name: semaphorin III/D-null targeting mice; code no. RBRC01104) and The Jackson Laboratory (strain name: B6;129P2-*Sema3f*^{tm1Mom}/MomJ; code no. 006710), respectively. A panel of 141 validated SNP (single nucleotide polymorphism) markers spaced evenly throughout the genome and covering all autosomes and the X chromosome[3, 4] was employed to define the percentage of C57Bl/6 and 129P2/OlaHsd genetic background of our *Sema3f* $^{+/-}$ mouse colony. The analysis showed that the genetic background of the *Sema3f* $^{+/-}$ mouse strain employed in our study was 91.5 ± 0.01413% C57Bl/6 and 8.5 ± 0.01413% 129P2/OlaHsd (Suppl. Fig. S1).

Single heterozygous mice (n=460 for *Sema3a* $^{+/-}$ and n=465 for *Sema3f* $^{+/-}$) were bred to examine the progeny of these mutants. To obtain double *Sema3a* $^{+/-}$/*Sema3f* $^{+/-}$ heterozygotes, single *Sema3a* $^{+/-}$ and *Sema3f* $^{+/-}$ mice were bred and a total of 405 pups were examined at birth. Genotyping was carried out by genomic PCR (polymerase chain reaction) of DNA samples extracted from tail tips following standard protocols. To obtain mouse embryos of defined gestational ages, heterozygous female mice in estrus were placed with heterozygous males in the evening. The morning of vaginal plug detection was defined as 0.5 dpc (days post-coitum). Embryos and yolk sacs were carefully dissected free of maternal tissue. Genomic DNA from yolk sac or embryos was analyzed by PCR (polymerase chain reaction) to determine the genotype. All animal procedures were approved by the Ethical Commission of the University of Torino and by the Italian Ministry of Health in compliance with the international laws and policies.

Isolation of Embryos and Yolk Sacs and Whole Mount Immunofluorescence Staining

Embryos and yolk sacs were removed from pregnant females at 9.5 and 10.5 dpc (days post-coitum) and examined. For whole-mount immunofluorescence staining, freshly dissected tissues were fixed for 2 hours in 4 %(PFA) paraformaldehyde at 4°C, washed in PBT (PBS - phosphatase buffered solution-, 0.1 % Tween 20) and subjected to dehydration in increasing methanol concentration (50 %, 80 % methanol/PBT, 100 % methanol) followed by rehydration in decreasing methanol concentration (80 %, 50 % methanol/PBT, PBT). After washing in Pblec (PBS - phosphatase buffered solution - pH 6.8, 1 % Tween 20, 1mM $CaCl_2$, 1mM $MgCl_2$, 0,1mM $MnCl_2$) embryos and yolk sac were incubated overnight with Rat-anti Endomucin (clone V.7C7 Santa Cruz sc-65495) diluted 1:20 in Pblec. After 5 washes in PBT, tissues were incubated overnight at 4°C with goat anti-rat Alexa 555 (Invitrogen) diluted 1:400 in PBT, followed by washing in PBT and post-fixation in 2 % PFA before analysis. Stained embryos and yolk sacs were photographed either and analyzed with a Leica TCS SP2 AOBS confocal laser-scanning microscope (Leica Microsystems).

In Vitro Generation of Model of VYS (visceral yolk sac) Eps (epithelial cells) From F9 Testicular Teratocarcinoma Stem Cells

Mouse testicular epithelium F9 cells (ATCC CRL-1720) were differentiated in VYS (visceral yolk sac) Eps (epithelial cells) as previously described[5, 6]. Briefly, F9 cells were grown in Dulbecco's Modified Eagle's Medium (D5546, Sigma Aldrich) supplemented with 10% of Fetal Bovine Serum (ECS0180D, EuroClone) and seeded in cell culture dishes, pre-coated with 0.1%

gelatin from porcine skin (G9136, Sigma Aldrich). F9 cells were differentiated into VYS (visceral yolk sac) Eps (epithelial cells), growing them in suspension in Bacteriological Petri dishes (#351029, Falcon, Corning Life Sciences Catalog), in presence of 50nmol/l Retinoic Acid (R2625, Sigma Aldrich) for 14 days. Culture medium was replaced every 2 days. After 14 days of culture, cells were collected in tubes, allowed to precipitate by gravity and stimulated or not with 800ng/ml recombinant mouse Sema3F (Semaphorin 3F), for different time points.

Immunofluorescence and Confocal Microscopy Quantification

Yolk sacs from E9.5 and mouse embryos were fresh frozen in OCT and 10µm-thick sections were cut using a Leica CM1900 cryostat. Sections were air-dried and fixed with Zinc Fixative (6,05g Tris, 0,35g $Ca(C_2H_3O_2)_2$, 2,5g $Zn(C_2H_3O_2)_2$, 2,5g $ZnCl_2$, 3,8 ml HCl 37 %) for 10 minutes at room temperature. Tissues were stained by employing the following primary antibodies: anti-Semaphorin 3F (ab39956, 1:100, Abcam), anti- Neuropilin-2 (AF567, 1:100, R&D Systems), anti-Myc (phospho-Thr58) (ab28842, 1:100, Abcam), anti-Myc (#5605, 1:100, Cell Signaling), anti-Thrombospondin-1 (LS-C137099, 1:100, Lifespan Biosciences), anti-Endomucin (clone V.7C7 Santa Cruz sc-65495), anti-Snail1 (sc-28199, 1:100, Santa Cruz Biotechnology) and anti-Cytokeratin 8/18 (GP11, PROGEN Biotechnik GmbH). To reveal phosphorylated VEGF-R2 in vascular EnCs, sections were incubated O/N at 4°C with purified Rabbit monoclonal anti-phospho-VEGF-R2 (Tyr1175) (clone 19A10, cat # 2478, Cell Signaling, dil. 1:100), anti-VEGF-R2 (cat # 55B11, Cell Signaling, dil. 1:100), anti-Thrombospondin-2 (LS-C393305, 1:100, Lifespan Biosciences), anti-Semaphorin 3A (cat #AF1250, R&D Systems, dil. 1:50) and purified Rat anti-endomucin (clone V.7C7 Santa Cruz sc-65495); anti-Rat Alexa Fluor-488 and anti-Rabbit Alexa Fluor-555 (dil. 1:400, Molecular Probes) were employed as secondary antibodies.

All tissue immunofluorescence images were captured by using a Leica TCS SP2 AOBS confocal laser-scanning microscope (Leica Microsystems) and by maintaining the same laser power, gain and offset settings. To determine the expression level of Myc and Thbs-1 proteins, we analyzed at least 2 non-overlapping fields for each yolk sac (n=6). Quantification was done by calculating the ratio between the red channel and the blue channel (Dapi - 4',6-diamidino-2-phenylindole) by means of ImageJ software. Data are presented as relative fold change of the total amount of Myc or Thbs-1 (thrombospondin 1) fluorescence normalized on the total cell number. Colocalization analysis was performed using plugins embedded in the visualization and analysis software ImageJ. Analysis was performed on a similar-sized symmetrical ROI (region of interest) selected for each dye. Background levels were subtracted from each ROI (region of interest) before calculating the degree of colocalization.

VYS (visceral yolk sac) Eps (epithelial cells) generated in vitro from F9 cells were either fixed in 4% paraformaldehyde for 20 min at room temperature or in cold methanol for 10 min at room temperature and permeabilized in PBS (phosphatase buffered solution) 0.5% Triton X-100 for 30 min or fixed in cold acetone for 2 min at room temperature and permeabilized in PBS (phosphatase buffered solution) 0.5% Triton X-100 for 15 min, in constant rotation. Cells were incubated with primary antibodies, diluted in PBS (phosphatase buffered solution) 0.2% Triton X-100, 1% DS (Donkey Serum) and maintained in constant rotation over-night at 4°C. Cells were washed with PBS (phosphatase buffered solution) 0.2% Triton X-100, 1% DS and incubated with the appropriate Alexa-Fluor-tagged secondary antibody for 2 hours at 4°C in constant rotation, protected from light. Cells were washed with PBS (phosphatase buffered solution) 0.2% Triton X-100, 1% DS and PBS (phosphatase buffered solution), included in Fluoromount-G Slide Mounting Medium (Cat. No. 0100-01, SouthernBiotech) and mounted on

microscope slides. Cells were analyzed by using a Leica TCS SP8 AOBS confocal laser-scanning microscope (Leica Microsystems).

RNA Preparation and Quantitative RT-PCR (quantitative reverse time polymerase chain reaction)

Littermate's embryos and yolk sacs (E9.5) were dissected and stored in RNAlater® reagent (QUIAGEN) over night at 4°C and then stored at -80°C. Total RNA was extracted using TRIzol® (Gibco-BRL; Grandisland, NY, USA) according to the manufacturer's recommendations. RNA amount was measured with a NanoDrop™ 1000 spectrophotometer (Thermo Scientific) under 260 nm. Two micrograms of total RNA was reverse transcribed to first strand complementary DNA (cDNA) using Random Primers and High-Capacity cDNA Reverse Transcription Kit (4368814 Life Technologies). cDNA was analyzed by TaqMan® gene expression single assay (Life technologies) by using the probe for *Vegfa* (Mm00437306_m1), *Thbs1*(Mm01335418) and ABI PRISM® 7900HT Fast Real-Time PCR System (Applied Biosystems). The data where analyzed by SDS and RQ Manager Software to obtain a relative quantification based on the arithmetical equation $2^{-\Delta\Delta Ct}$, in which ΔΔCt is the normalized signal level in a sample relative to the normalized signal level in the corresponding calibrator sample. mRNAs were normalized to the housekeeping *tbp* and the fold changes (RQ) were calculated compared with the ΔCt of wild type embryos and yolk sacs.

Yolk Sac miRNAs Extraction and Expression Profiling

Six E9.5 yolk sacs for each experimental group (wild type, *Sema3f* $^{-/-}$, and *Sema3a* $^{-/-}$ embryos) were pooled and used for miRNAs extraction. MiRNAs were isolated using the mirVana™ miRNA Isolation Kit (Ambion) according to the manufacturer's instruction. The purity and quantity of RNAs were assessed by means of the Nanodrop™ 1000 spectrophotometer (Thermo Scientific). All samples were diluted to have a total of 2 μg in a final volume of 10μl. Samples were used immediately or stored at -80°C for future use. Mouse miRNAs for mmu-miR-18a and mmu-miR-19b-1 were analyzed with technical triplicate by using quantitative RT-PCR (reverse transcription polymerase chain reaction) with specific probes.

Histology and Immunohistochemistry of Mouse Placentas.

10.5 days of gestational age placentas were collected, fixed in buffered formalin and embedded in paraffin. Serial sagittal sections of 5 μm were sectioned using a Leica 2135 microtome. Every 5th slide was deparaffinized and subjected to graded rehydration through xylene, 100 %, 95 %, 70 % ethanol and then stained with hematoxylin and eosin (H&E) as previously described (Fisher et al., 2008). Slides were examined in order to find the midpoint of the placenta (site of umbilical attachment), which is used as the major reference point for comparisons between mutants and wild type littermates. For immunostaining, the same formalin-fixed placentas were sectioned at 3μm and slides were incubated with 3 % H_2O_2 for 20 minutes to suppress the endogenous peroxidase activity. After 3 washes in Phosphatase Buffered Solution (PBS), slides were immersed in diluted Dako Target Retrieval Solution (S1699) and heated in a water bath (95-96°C). Sections were probed over night with rat-anti Endomucin (clone V.7C7 Santa Cruz sc-65495) diluted 1: 50 in blocking solution (Dako, X0909). After 3 washes in PBS, slides were incubated for 1 hour at room temperature with the polyclonal rabbit anti-rat immunoglobulins conjugated with horseradish peroxidase (Dako). The signal was detected by using the Dako AEC (K3461) and the slides were mounted with the Dako Mounting Medium (CS703). Images were

captured with a BX-60 microscope (Olympus) equipped with a color Qicam Fast 1394-digital CCD camera 12 bits (QImaging Corp.) and analyzed by the Image-Pro Plus 6.2 Software (Media Cybernetics).

Blood vessels branching analysis

Quantification of vessel branching was obtained by analyzing the placenta of wild type (n=3), *Sema3a* $^{-/-}$ (n=3), and *Sema3f* $^{-/-}$ (n=3) mice. At least three 10x power field immunohistochemical images were analyzed for each sample. Images were processed by means of ImageJ open source software (http://imagej.net/Home). Immunohistochemically stained blood vessel networks were separated by means of the ImageJ color deconvolution plugin. The resulting black and white images were imported into the imaging software winRHIZO Pro (Regent Instruments Inc.) and analyzed as previously described [7]

Statistical Analysis

Results of all experiments are expressed as mean ± SD or SEM. Statistical analyses were performed using 2-tailed heteroscedastic Student *t*-test using GraphPad Prism software. A p value below 0.05 was considered significant.

References

1. Taniguchi M, Yuasa S, Fujisawa H, Naruse I, Saga S, Mishina M, Yagi T. Disruption of semaphorin iii/d gene causes severe abnormality in peripheral nerve projection. *Neuron*. 1997;19:519-530.

2. Walz A, Feinstein P, Khan M, Mombaerts P. Axonal wiring of guanylate cyclase-d-expressing olfactory neurons is dependent on neuropilin 2 and semaphorin 3f. *Development*. 2007;134:4063-4072

3. Petkov PM, Ding Y, Cassell MA, Zhang W, Wagner G, Sargent EE, Asquith S, Crew V, Johnson KA, Robinson P, Scott VE, Wiles MV. An efficient snp system for mouse genome scanning and elucidating strain relationships. *Genome Res*. 2004;14:1806-1811

4. Petkov PM, Cassell MA, Sargent EE, Donnelly CJ, Robinson P, Crew V, Asquith S, Haar RV, Wiles MV. Development of a snp genotyping panel for genetic monitoring of the laboratory mouse. *Genomics*. 2004;83:902-911

5. Hogan BL, Taylor A, Adamson E. Cell interactions modulate embryonal carcinoma cell differentiation into parietal or visceral endoderm. *Nature*. 1981;291:235-237

6. Thompson JR, Gudas LJ. Retinoic acid induces parietal endoderm but not primitive endoderm and visceral endoderm differentiation in f9 teratocarcinoma stem cells with a targeted deletion of the rex-1 (zfp-42) gene. *Mol Cell Endocrinol*. 2002;195:119-133

7. Maione F, Molla F, Meda C, Latini R, Zentilin L, Giacca M, Seano G, Serini G, Bussolino F, Giraudo E. Semaphorin 3a is an endogenous angiogenesis inhibitor that blocks tumor growth and normalizes tumor vasculature in transgenic mouse models. *J Clin Invest*. 2009;119:3356-3372

Supplemental Information

Sema3F (Semaphorin 3F) Selectively Drives an Extraembryonic Proangiogenic Program

Donatella Regano, Alessia Visintin, Fabiana Clapero, Federico Bussolino, Donatella Valdembri, Federica Maione, Guido Serini and Enrico Giraudo

Supplementary Results

Since *Sema3f*-null yolk sacs were poorly vascularized, next we analyzed the vascularization of the placenta that constitutes the second crucial extraembryonic organ in the control of nutrient and gas exchanges. In the mouse, placenta development, is usually complete by E12.5 [1]. Proceeding from the fetal to the maternal side, the mature placenta consists of the labyrinth, the spongiotrophoblast, and the uterine decidua [2]. Due to the abundant vascularization, when viewed externally from the chorion side, the labyrinth of E9.5 wild type mice placentas was bright red and the labyrinth edge was easily discernible (Figure IIA). While placentas of E9.5 *Sema3a*null mice did not exhibit gross alteration (Figure IIG), those of *Sema3f* $^{-/-}$ mice were instead very anemic (Figure IID), suggesting the likely presence of labyrinth abnormalities. Indeed, if compared to wild type (Figure IIB) and *Sema3a* $^{-/-}$ (Figure IIH) counterparts, in E10.5 *Sema3f* $^{-/-}$ placentas (Figure IIE) all layers were present, but the labyrinth layer thickness was almost halved, the maternal blood filled lacunae were absent, and the spongiotrophoblast layer was markedly thinner. Accordingly, *Sema3f* $^{-/-}$ (Figure IIF), but not wild type (Figure IIC) and *Sema3a* $^{-/-}$ (Figure III) placentas displayed a dramatic reduction in endomucin-stained labyrinth blood vessels (Figure IIF). Notably, in line with the effect of Sema3A (Semaphorin 3A) in regulating blood vessel remodeling, the branching of the vasculature of *Sema3a* $^{-/-}$, but not *Sema3f* $^{-/-}$ placentas was significantly increased compared to controls (1.8-fold, Figure IIJ).

Supplementary Discussion

Several studies previously investigated the role of Sema3F (Semaphorin 3F) in peripheral and central nervous system development [3-9]. More recently, Uchida and colleagues highlighted the role of Sema3F as an inhibitor of lymphatic vessel development in the mouse embryo [10]. Here, we report instead for the first time the analysis of the role of Sema3F in the development of blood vessels in the murine embryo and associated extraembryonic organs. We discovered that, differently from all the inhibitory effects described so far either in the nervous or in the lymphatic system, surprisingly and unpredictably Sema3F acts as a key promoter of developmental angiogenesis only in extraembryonic organs, namely yolk sac and placenta, with potential implications for life-threatening human diseases, such as pre-eclampsia. Indeed, Zhou and colleagues [11] previously reported how placental cytotrophoblasts of human preeclampsia patients express abnormally high levels of Nrp2-binding SEMA3B (SEMAPHORIN 3B) that, by inhibiting cytotrophoblasts motility and angiogenesis, participates to the pathogenesis of this disease. We provide evidence of how Nrp2 (Neuropilin 2)-binding Sema3F activates instead crucial signals that promote extraembryonic angiogenesis and placental development. Altogether these findings suggest that Nrp2-binding SEMA3B and SEMA3F (SEMAPHORIN 3F) proteins may be involved in both physiological and pathological placental development and may represent actionable targets for therapeutic intervention in preeclampsia.

Supplementary Figure Legends

Figure I. SNP (single nucleotide polymorphism) characterization of the genetic background of the Sema3f heterozygous strain. The genomic DNA of 11 *Sema3f*$^{+/-}$ mice (Test01-11) was analyzed to determine the percentage of C57BL/6 and 129P2/OlaHsd genetic background by using a panel of 141 validated SNP markers (SNP_ID) spaced evenly throughout the genome and covering all autosomes and the X chromosome. Genomic DNA of pure C57BL/6 (Ctl01) and 129P2/OlaHsd (Ctl02) mice as well as that of a heterozygous C57BL/6 / 129P2/OlaHsd (Ctl03) mice were employed for control purposes. The analysis showed that the genetic background of the *Sema3f*$^{+/-}$ mouse strain was 91.5 ± 0.01413% C57BL/6 and 8.5 ± 0.01413% 129P2/OlaHsd.

Figure II. Sema3 (class 3 semaphorin)-F is required for placental blood vessel formation. Stereomicroscopic images of E10.5 wild type (**A**), *Sema3f* $^{-/-}$ (**D**) and *Sema3a* $^{-/-}$ (**G**) placentas. On the chorion side, the bright red edge of the labyrinth is easily discernible in E10.5 wild type and *Sema3a* $^{-/-}$, but not *Sema3f* $^{-/-}$ placentas that are poorly vascularized. Hematoxylin-eosin stained histological sections of placental tissues of E10.5 wild type (**B**), *Sema3f* $^{-/-}$ (**E**) and *Sema3a* $^{-/-}$ (**H**) placentas. If compared to wild type (**B**) and *Sema3a* $^{-/-}$ (**H**) samples, *Sema3f* $^{-/-}$ placentas (**E**) are characterized by a significant reduction in size of Sp (spongiotrophoblast) and La (labyrinth) layers. Endomucin immunohistochemical staining reveals that wild type (**C**), but not *Sema3f* $^{-/-}$ placentas (**F**) display an extensive and vascularized labyrinth network. While no gross alterations in the vessels density were observed in the labyrinth layer of *Sema3a* $^{-/-}$ placentas (**I**). Analysis of endomucin-stained placenta revealed a 1.8 increase in blood vessel branching in *Sema3a*$^{-/-}$ (n=3), but not *Sema3f* $^{-/-}$ mice (n=6) (**J**). GI (giant cells into the uterin decidua). Scale bars, 100 μm (**A**, **D**, **G**) and 200 μm (**B**, **C**, **E**, **F**, **H**, **I**). ** $p<0.001$.

Figure III. A, Sema3(class 3 semaphorin)-A expression is not affected in *Sema 3f*$^{-/-}$ yolk sacs and it largely co-localizes with endomucin^{+} EnCs (endothelial cells). **B**, Bar graph shows the percentage of Sema3A colocalization with endomucin both in wild type and *Sema 3f*$^{-/-}$ yolk sacs. **C**, In E9.5 embryos, Sema3F is mainly expressed by endomucin^{+} EnCs of both wild type and *Sema3a* $^{-/-}$ embryos. As expected, Sema3F protein is undetectable in *Sema 3f*$^{-/-}$ embryos. Scale bars, 100 μm. **D**, Bar graph shows the percentage of Sema3F co-localization with endomucin both in wild type and mutant embryos.

Figure IV. Sema3 (class 3 semaphorin)-F promotes Thbs1 (thrombospondin 1) gene transcription in the mouse yolk sac while does not affect Vegfa transcription**. A**, RT-PCR (reverse transcription polymerase chain reaction) on wild type and *Sema3f* $^{-/-}$ yolk sacs did not display a significant difference in *Vegfa* mRNA transcription level. (*n=6*). **B**, RT-PCR (reverse transcription polymerase chain reaction) analysis reveals how, compared to wild type yolk sacs, *Thbs1* mRNA increases in *Sema3f* $^{-/-}$ yolk sacs and decreases in *Sema3a* $^{-/-}$ yolk sacs (* $p<0.05$).

Figure V. Sema3f -knockdown does not affect Thbs2 (thrombospondin 2) protein expression. **A** Quantification of immunofluorescence analysis of E9.5 yolk sacs showed that Thbs2 protein is mainly expressed in CK8/18 (cytokeratin 8/18) $^{+}$ VYS (visceral yolk sac) EpCs (epithelial cells). No differences in Thbs2 expression were observed in *Sema3f* $^{-/-}$ yolk sacs compared to wild type controls. **B**, Bar graph shows the percentage of Thbs2 colocalization with endomucin, CK8/18, and Snail1 both in wild type and *Sema3f*$^{-/-}$ yolk sacs. Scale bars, 100 μm.

Figure VI. Sema3F (Semaphorin 3F) promotes extraembryonic angiogenesis: a working model**.**

Supplementary References

1. Maltepe E, Fisher SJ. Placenta: The forgotten organ. *Annu Rev Cell Dev Biol*. 2015;31:523-552
2. Watson ED, Cross JC. Development of structures and transport functions in the mouse placenta. *Physiology (Bethesda)*. 2005;20:180-193
3. Sahay A, Molliver ME, Ginty DD, Kolodkin AL. Semaphorin 3f is critical for development of limbic system circuitry and is required in neurons for selective cns axon guidance events. *J Neurosci*. 2003;23:6671-6680
4. Cloutier JF, Sahay A, Chang EC, Tessier-Lavigne M, Dulac C, Kolodkin AL, Ginty DD. Differential requirements for semaphorin 3f and slit-1 in axonal targeting, fasciculation, and segregation of olfactory sensory neuron projections. *J Neurosci*. 2004;24:9087-9096
5. Gammill LS, Gonzalez C, Gu C, Bronner-Fraser M. Guidance of trunk neural crest migration requires neuropilin 2/semaphorin 3f signaling. *Development*. 2006;133:99-106
6. Yamauchi K, Mizushima S, Tamada A, Yamamoto N, Takashima S, Murakami F. Fgf8 signaling regulates growth of midbrain dopaminergic axons by inducing semaphorin 3f. *J Neurosci*. 2009;29:4044-4055
7. Kolk SM, Gunput RA, Tran TS, van den Heuvel DM, Prasad AA, Hellemons AJ, Adolfs Y, Ginty DD, Kolodkin AL, Burbach JP, Smidt MP, Pasterkamp RJ. Semaphorin 3f is a bifunctional guidance cue for dopaminergic axons and controls their fasciculation, channeling, rostral growth, and intracortical targeting. *J Neurosci*. 2009;29:12542-12557
8. Demyanenko GP, Mohan V, Zhang X, Brennaman LH, Dharbal KE, Tran TS, Manis PB, Maness PF. Neural cell adhesion molecule nrcam regulates semaphorin 3f-induced dendritic spine remodeling. *J Neurosci*. 2014;34:11274-11287
9. Coate TM, Spita NA, Zhang KD, Isgrig KT, Kelley MW. Neuropilin-2/semaphorin-3f-mediated repulsion promotes inner hair cell innervation by spiral ganglion neurons. *Elife*. 2015;4
10. Uchida Y, James JM, Suto F, Mukouyama YS. Class 3 semaphorins negatively regulate dermal lymphatic network formation. *Biol Open*. 2015;4:1194-1205
11. Zhou Y, Gormley MJ, Hunkapiller NM, Kapidzic M, Stolyarov Y, Feng V, Nishida M, Drake PM, Bianco K, Wang F, McMaster MT, Fisher SJ. Reversal of gene dysregulation in cultured cytotrophoblasts reveals possible causes of preeclampsia. *J Clin Invest*. 2013;123:2862-2872

Figure I. *Single nucleotide polymorphism (SNP) characterization of the genetic background of the Sema3f heterozygous strain.*

			C57BL/6J	251/278	260/282	251/276	245/276	257/282	255/280	253/278	250/274	257/276	265/282	257/278	280/280	/282	141/282
			129P2/OlaHsd	27/278	22/282	25/276	31/276	25/282	25/280	25/278	24/274	19/276	17/282	21/278	/280	282/282	141/282
			C57BL/6J	90.29%	92.20%	90.94%	88.77%	91.13%	91.07%	91.01%	91.24%	93.12%	93.97%	92.45%	100.00%	0.00%	50.00%
			129P2/OlaHsd	9.71%	7.80%	9.06%	11.23%	8.87%	8.93%	8.99%	8.76%	6.88%	6.03%	7.55%	0.00%	100.00%	50.00%
			Sample	541 F1	473 F1	211 F2	248 F2	475 F2	340 D2	707 D2	40 D2	26 D3	49 D3	53 D3	B6J	129S	Het
SNP_ID	Expected SNPs																
Chromosome-bp	C57BL/6J	129S1/SvImJ		Test01	Test02	Test03	Test04	Test05	Test06	Test07	Test08	Test09	Test10	Test11	Ctl01	Ctl02	Ctl03
01-005230167-M	C	T		T	T/C		T	T/C	C	C	C	C	C	C	C	T	T/C
01-026072256-M	G	T		G	G	G	G	G	G	G	G	G	G	G	G	T	T/G
01-046003967-M	A	C		A	A	A	A	A	A	A	A	A	A	A	A	C	C/A
01-066294607-M	A	G		G/A	A	A	A	A	A	A	A	A	A	A	A	G	G/A
01-086182722-M	A	G		A	A	A	A	A	A	A	A	A	A	A	A	G	G/A
01-102073421-M	G	C		G	G	G	G	G	G	G	G	G	G	G	G	C	C/G
01-143006008-M	A	G		A	A	A	A	A	A	A		A	A	A	A	G	G/A
01-162977516-M	G	A		G	G	G	G	G	G	G	G	G	G	G	G	A	A/G
01-185013929-M	C	G		C	C	C	C	C	C	C	C	C	C	C	C	G	G/C
02-003179310-M	G	A		G	G	G	G	G	G	G	G		G	G	G	A	A/G
02-020551513-M	A	G		A	A	A	A	A	A		A	A	A	A	A	G	G/A
02-040184477-M	C	T		C	C	C	C	C	C	C	C	C	C	C	C	T	T/C
02-061161692-M	T	C		T	T	T	T	T	T	T	T	T	T	T	T	C	C/T
02-078062303-M	T	G		T	T	T	T	T	T	T	T	T	T	T	T	G	G/T
02-104075364-M	G	C		G	G	G	G	G	G	G	G	G	G	G	G	C	C/G
02-119931810-M	A	T			T/A	T/A	T	T/A	A	A	A	A	A	A	A	T	T/A
02-139603599-M	T	A		T	T	T	T	T	T	T	T	T	T	T	T	A	A/T
02-160869410-N	T	C		C	T/C	T/C	C	T/C	T	T	T	T	T	T	T	C	T/C
02-179086475-M	G	T		G	G	G	G	G	G	G	G	G	G	G		T	T/G
03-011350737-M	G	C		G	G	G	C/G	G	G	C/G	G	G	G	G	G	C	C/G
03-031231243-M	T	C		T	C/T	T	C/T	C/T	T	T		T	T	T	T	C	C/T
03-062390782-M	G	A		A	A	A	A	A	A	A/G	A	A	A	A	G	A	A/G
03-082192100-M	G	A		A	A/G	A/G	A	A	A/G	G	A/G	A/G	A	A	G	A	A/G
03-102189723-M	T	G															
03-119173143-M	G	A		G	G	G	G	G	G	G	G	G	G	G	G	A	A/G
03-139158872-M	G	A		G	G	G	G	G	G	G	G	G	G	G	G	A	A/G
03-160287200-M	G	A		G	A/G	A/G	G	A/G	A	A	A	A	A	A	G	A	A/G
04-003163167-M	G	T		G	G	G	G	G	G	G	G	G	G	G	G	T	T/G
04-024192594-M	T	A		T	T	T	T	T	T	T	T	T	T	T	T	A	A/T
04-046000627-M	A	T		A	A	A	A	A	A	A	A	A	A	A	A	T	T/A
04-067425585-N	T	C		T	T	T	T	T	T	T	T	T	T	T	T	C	C/T
04-086758585-N	A	G		A	A	A	A	A	A	A	A	A	A	A	A	G	G/A
04-106314110-M	C	A		C	C	C	C	C	C	C		C	C	C	C	A	A/C
04-125988404-M	T	A		T	T	T	T	T	T	T	T	T	T	T	T	A	A/T
04-145870512-M	C	G		C	C	C	C	C	C	C	C	C	C	C	C	G	G/C
05-009080098-M	G	A		G	G	G	G	G	G	G	G	G	G	G	G	A	A/G
05-029064177-N	A	G		A	A	A	A	A	A	A	A	A	A	A	A	G	A/G
05-049570566-N	G	T		G	G	G	G	G	G	G	G	G	G	G	G	T	T/G
05-069043957-M	A	G		A	A	A	A	A	A	A	A	A	A	A	A	G	G/A
05-088937905-M	G	A		G	G	G	G	G	G	G	G	G	G	G	G	A	A/G
05-107871207-M	G	A		G	G	G	G	G	G	G	G	G	G	G	G	A	A/G
05-128944450-M	T	C		T	T	T	T	T	T	C/T	T	T	T	T	T	C	C/T
05-130950804-M	A	C		A	A	A	A	A	A		A	A	A	A	A	C	C/A
05-149044358-M	C	A		C	C	C	C	C	C	C	C	C	C	C	C	A	A/C
06-003167392-M	C	T		C	C	C	C	C	C	C	C	C	C	C	C	T	T/C
06-020075608-M	T	G		T	T	T	T	T	T	T	T	T	T	T	T	G	G/T
06-036801292-N	T	C		T	T	T	T	T	T	T	T	T	T	T	T	C	T/C
06-056162117-M	A	G		G	A	A	G/A	A	A	A	A	A	A	A	A	G	G/A
06-076285738-M	T	A		T	T	T	T	T	T	T	T	T	T	T	T	A	A/T
06-084009195-M	A	G		A	A	A	A	A	A	A	A	A	A	A	A	G	G/A
06-122941044-M	T	A		T	T	T	T	T	T	T	T	T	T	T	T	A	A/T
06-146079591-M	A	C		A	A	A	A	A	A	A	A	A	A	A	A	C	C/A
07-004201219-N	A	G		A	A	A	A	A	A	A	A	A	A	A	A	G	G/A

07-022997618-M	C	T		C	C	C	C	C	C	C	C	C	C	C	C	C	T	T/C
07-041032053-M	G	A		G	G	G	G	G	G	G	G	G	G	G	G	G	A	A/G
07-061010042-M	C	T		C	C	C	C	C	C	C	C	C	C	C	C	C	T	T/C
07-080974545-M	T	G		T	T	T		T	T	T	T	T	T	T	T	T	G	G/T
07-102009856-M	C	T		C	C	C	C	C	C	C	C	C	C	C	C	C	T	T/C
07-124090029-M	A	G		A	A	A	A	A	A	A	A	A	A	A	A	A	G	G/A
08-003089774-M	T	C		T	T	T	T	T	T	T	T	T	T	T	T	T	C	C/T
08-022074356-M	A	G		A	A	A	A	A	G/A	A	G/A	G	G/A		A	A	G	G/A
08-041947937-M	T	A		T	T	T	T	T		T	A	A/T	A/T	A	T	A	A	A/T
08-067470102-N	G	C		G	G	G	G	G	G	G	G	G	G	G	G	G	C	G/C
08-086985036-M	C	T		C	C	C	C	C	C	C	C	C	C	C	C	C	T	T/C
08-107088585-M	A	G		A	A	A	A	A	G/A	A	A	A	A	A	A	A	G	G/A
08-123021323-M	T	C		T	T	T	T	T	T	T	T	T	T	T	T	T	C	C/T
09-005920375-M	G	A		G	G	G	G	G	G	G	G	G	G	G	G	G	A	A/G
09-027092605-M	T	G		T	T	T	T	T	T	T	T	T	T	T	T	T	G	G/T
09-046117336-N	A	G		A	A	A	A	A	A	A	A	A	A	A	A	A	G	G/A
09-066767939-N	G	A		G	G	G	G	G	G	G	G	G/A	G/A	G	G	A	G	G/A
09-086008489-M	A	C		A	A	A	A	A	A	C/A	A	A	A	A	A	C	C	C/A
09-106854728-M	C	T		C	C	C	C	C	C	C	C	C	C	C	C	C	T	T/C
09-125082704-M	G	A		G	G	G	G	G	G	G	G	G	G	G	G	G	A	A/G
10-006702399-N	A	T		A	A	A	A	A	A	A	A	A	A	A	A	A	T	A/T
10-027070647-M	G	T		G	G	G	G	G	G	G	G	G	G	G	G	G	T	T/G
10-045078228-M	A	G		A	A	A	A	A	A	A	A	A	A	A	A	A	G	G/A
10-053898997-M	G	C		G	G	G	G	G	G	G	G	G	G	G	G	G	C	C/G
10-092128703-M	G	A		G	G	G	G	G	G	G	G	G	G	G	G	G	A	A/G
10-107333522-M	C	T		T/C	C	C	T	T/C	C	C	C	C	C	C	C	C	T	T/C
10-127241589-M	G	A		G	G	G	G	G	G	G	G	G	G	G	G	G	A	A/G
11-004367508-M	G	A		A/G	A/G	G	A/G	A/G	G	G	G	G	G	G	G	G	A	A/G
11-024515722-M	G	A		G	G	G	G	G	G	G	G	G	G	G	G	G	A	A/G
11-044333996-M	A	G		A	A	A	A	A	A	A	A	A	A	A	A	A	G	G/A
11-063538723-N	G	A		G	G		G	G	G	G	G	G	G	G	G	G	A	G/A
11-083523677-M	G	C		G	G	G	G	G	G	G	G	G	G	G	G	G	C	C/G
11-104171075-M	A	G		A	A	A	A	A	A	A	A	A	A	A	A	A	G	G/A
11-108428031-M	T	C		T	T	T	T	T	T	T	T	T	T	T	T	T	C	C/T
11-111226923-M	A	C			C/A	C/A	A	C/A	C/A	A	A	A	A	A	A	A	C	C/A
11-122195777-M	C	T		C	C	C	C	C	C	C	C	C	C	C	C	C	T	T/C
12-003567042-M	G	T		G	G	G	G	G	G	G	G	G	G	G	G	G	T	T/G
12-024149189-N	T	C		T	T	T	T	T	T	T	T	T	T	T	T	T	C	T/C
12-045157254-N	C	T		C	C	C	C	C	C	C	C	C	C	C		C	T	T/C
12-065480669-M	C	T		C	T	T/C	C	T/C	T	T	T	T	T	T	T	C	T	T/C
12-084289638-M	C	A		A	C	A/C	A/C	A/C	A/C	A/C	A/C		A/C	A	C	A	A/C	
12-099072867-M	T	C		T	T	T	C/T	T	C/T	T	C/T	T	C/T	T	T	C	C/T	
12-113315003-M	C	G		C	C	C		C	C	C	C	C	C	C	C	G	G/C	
13-009820324-M	A	G		A	A		A	A	A	A	A	A	A	A	A	G	G/A	
13-030913320-M	T	C		T	T	T	T	T	T	T	T	T	T	T	T	C	C/T	
13-052501751-N	G	A		G	G	G	G	G	G	G		G	G	G	G	A	A/G	
13-071928027-M	C	A		C	C	C	C	C	C	C	C	C	C	C	C	A	A/C	
13-091042598-M	G	A		G	G	G	G	G	G	G	G	G	G	G	G	A	A/G	
13-113057436-M	A	G		A	A	A	A	A	A	A	A	G/A	G/A	A	A	G	G/A	
14-005055006-M	T	A		T	T	T	T	T	T	T	T	T	T	T	T	A	A/T	
14-024063411-M	A	G		A	A	A	A	A	A	A	A	A	A	A	A	G	G/A	
14-043974306-M	T	A		T	T	T	T	T	T	T	T	T	T	T	T	A	A/T	
14-063983099-M	A	G		A	A	A	A	A	A	A	A	A	A	A	A	G	G/A	
14-074468555-M	G	A		G	G	G	G	G	G	G	G	G	G	G	G	A	A/G	
14-093080383-M	G	A		G	G	G	G	G	G	G	G	G	G	G	G	A	A/G	
14-112205439-N	G	A		G	G	G	G	G	G	G	G	G	G	G	G	A	A/G	
15-003094890-M	A	G		G/A	G	G/A	G/A	G/A	A	A	A	A	A	A	A	G	G/A	
15-020280219-M	G	T		G	G	G	G	G	G	T/G	G	G	G	G	G	T	T/G	
15-039906196-M	G	A		G	G	G	A/G	G	G	A/G	G	G	G	G	G	A	A/G	
15-059754938-N	C	T		T/C	C	T/C	T	C	C	C	C	C	C	C	C	T	T/C	
15-080211114-N	A	G		A/G	A	A/G	A/G	A/G	A	A	A	A	A	A	A	G	A/G	

15-098621793-N	C	T		C	C	C/T	C/T	C/T	C	C	C	C	C	C	C	T	C/T
16-005053446-C	G	T		T	G	G	T/G	T/G	T/G	G	T/G	G	G	G	G	T	T/G
16-019621494-C	A	G		A/G	A	A	A/G	A/G	A/G	A	G	A/G	A/G	A/G	A	G	A/G
16-037994236-C	G	A		G/A	G	A		G	G/A	G/A	G/A	G/A	G	G/A	G	A	G/A
16-057482753-C	A	G		A	A	A/G	A	A	A/G	G	A/G	A/G	A	A/G	A	G	A/G
16-075684315-C	T	C		T/C	T	T	T/C	T	T/C	C	T/C	T/C	T	T/C	T	C	T/C
16-095103053-C	C	G		C/G	C	C	C/G	C	C	C	C	C	C	C	C	G	C/G
17-004147924-M	A	G		A	A	A	A	A	A	A	A	A	A	A	A	G	G/A
17-024364775-M	G	A		G	G	G	G	G	G	G	G	G	G	G	G	A	A/G
17-043164647-M	G	A		G	G	G	G	G	G	G	G	G	G	G	G	A	A/G
17-066532305-N	T	G		T	T	T	T	G/T	G/T	G/T	T	T	G/T	G/T	T	G	G/T
17-086110517-N	G	A		G	G	G	G	G	G	G	G	G	G	G	G	A	A/G
18-005066417-M	T	C		T	T	T	T	T	T	T	T	T	T	T	T	C	C/T
18-030864114-M	T	C		C/T	C	C	T	T	C/T	C	C/T		T	C/T	T	C	C/T
18-049391366-N	T	C		T	C	C	T	T/C	T/C	C	C	T/C	T	T/C	T	C	T/C
18-070565016-N	C	T		T/C	T	T	T/C	T	T/C	T/C	T/C	T/C	T/C	T/C	C	T	T/C
18-090060367-M	G	T		G	G	G	G	G	G	G	G	G	G	G	G	T	T/G
19-021081804-M	A	G		A	G/A	G/A	A	G/A	G/A	G/A	A	A	A	A	A	G	G/A
19-041909356-M	G	A		G	G	G	G	G	A/G	A/G	G	G	G	G	G	A	A/G
19-060030696-N	A	G		G/A	G/A	G	G	G/A	G	G/A	G	G/A	A	G/A	A	G	G/A
X-008280846-M	A	G		A	A	A	A	A	A	A	A	A	A	A	A	G	G/A
X-035414447-M	T	C		T	T	T	T	T	T	T	T	T	T	T	T	C	C/T
X-054650362-N	T	A		T	T	T	T	T	T	T	T	T	T	T	T	A	A/T
X-068494838-M	C	T		C	C	C	C	C	C	C	C	C	C	C	C	T	T/C
X-088983795-M	T	C		T	T	T	T	T	T	T	T	T	T	T	T	C	C/T
X-109677875-M	A	G		A	A	A	A	A	A	A	A	A	A	A	A	G	G/A
X-123551831-M	A	G		A	A	A	A	A	A	A	A	A	A	A	A	G	G/A
X-143466659-M	A	C		A	A	A	A	A	A	A	A	A	A	A	A	C	C/A

Figure I. *Single nucleotide polymorphism (SNP) characterization of the genetic background of the Sema3f heterozygous strain.* The genomic DNA of 11 *Sema3f*$^{+/-}$ mice (Test01-11) was analyzed to determine the percentage of C57BL/6 and 129P2/OlaHsd genetic background by using a panel of 141 validated SNP markers (SNP_ID) spaced evenly throughout the genome and covering all autosomes and the X chromosome. Genomic DNA of pure C57BL/6 (Ctl01) and 129P2/OlaHsd (Ctl02) mice as well as that of a heterozygous C57BL/6 / 129P2/OlaHsd (Ctl03) mouse were employed for control purposes. The analysis showed that the genetic background of the *Sema3f*$^{+/-}$ mouse strain was 91.5 ± 0.01413% C57BL/6 and 8.5 ± 0.01413% 129P2/OlaHsd.

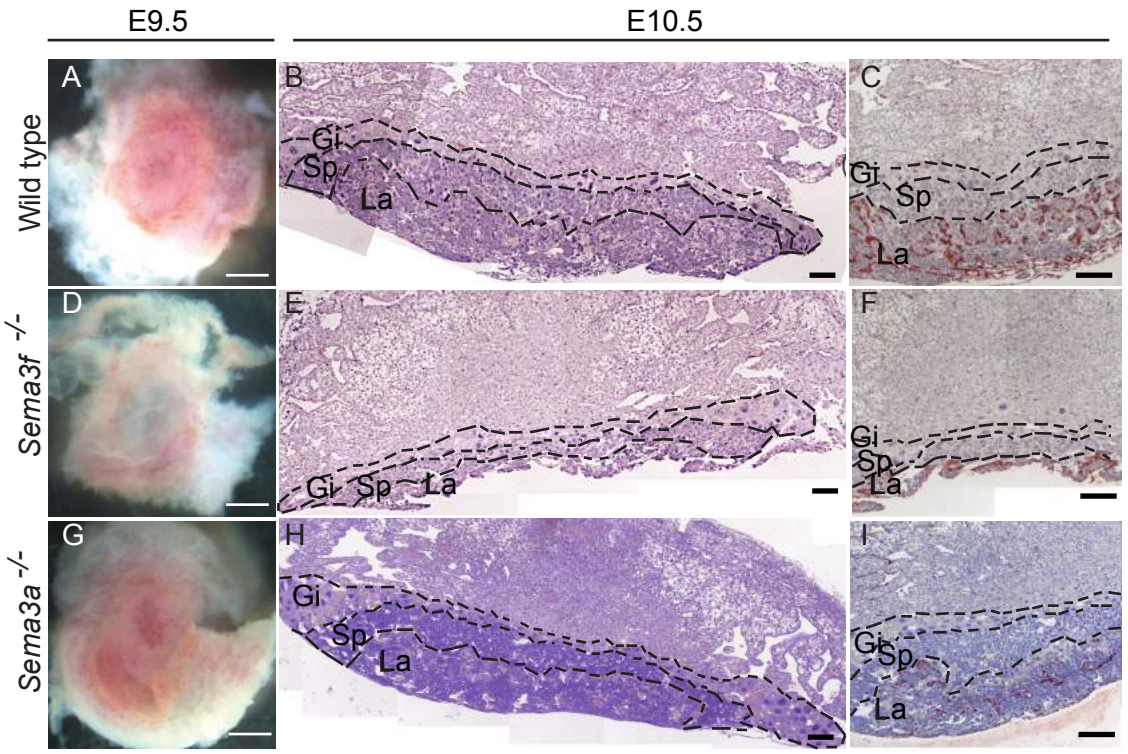

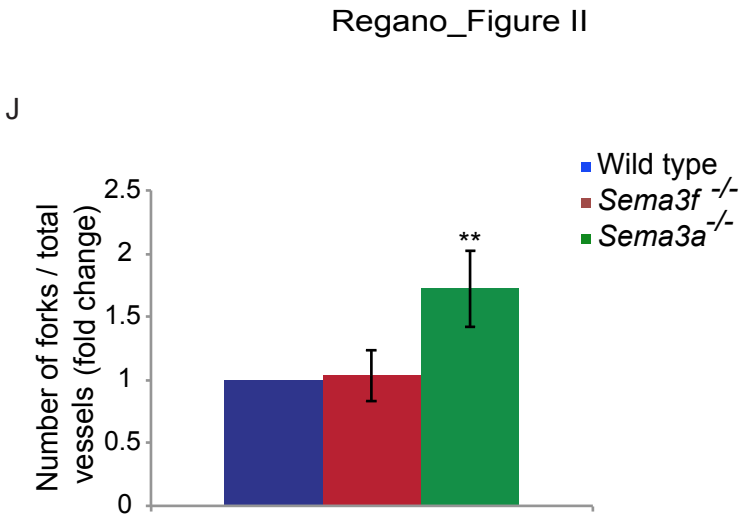

Figure II. Sema3 (class 3 semaphorin)-F is required for placental blood vessel formation. Stereomicroscopic images of E9.5 wild type (**A**), Sema3f $^{-/-}$ (**D**) and Sema3a $^{-/-}$ (**G**) placentas. On the chorion side, the bright red edge of the labyrinth is easily discernible in E10.5 wild type and Sema3a $^{-/-}$, but not Sema3f $^{-/-}$ placentas that are poorly vascularized. Hematoxylin-eosin stained histological sections of placental tissues of E10.5 wild type (**B**), Sema3f $^{-/-}$ (**E**) and Sema3a $^{-/-}$ (**H**) placentas. If compared to wild type (**B**) and Sema3a $^{-/-}$ (**H**) samples, Sema3f $^{-/-}$ placentas (**E**) are characterized by a significant reduction in size of Sp (spongiotrophoblast) and La (labyrinth) layers. Endomucin immunohistochemical staining reveals that wild type (**C**), but not Sema3f $^{-/-}$ placentas (**F**) display an extensive and vascularized labyrinth network. While no gross alterations in the vessels density were observed in the labyrinth layer of Sema3a $^{-/-}$ placentas (**I**). Analysis of endomucin-stained placenta revealed a 1.8 increase in blood vessel branching in Sema3a$^{-/-}$ (n=3), but not Sema3f $^{-/-}$ mice (n=6) (**J**). GI (giant cells into the uterin decidua). Scale bars, 100 μm (**A**, **D**, **G**) and 200 μm (**B**, **C**, **E**, **F**, **H**, **I**). ** p<0.001.

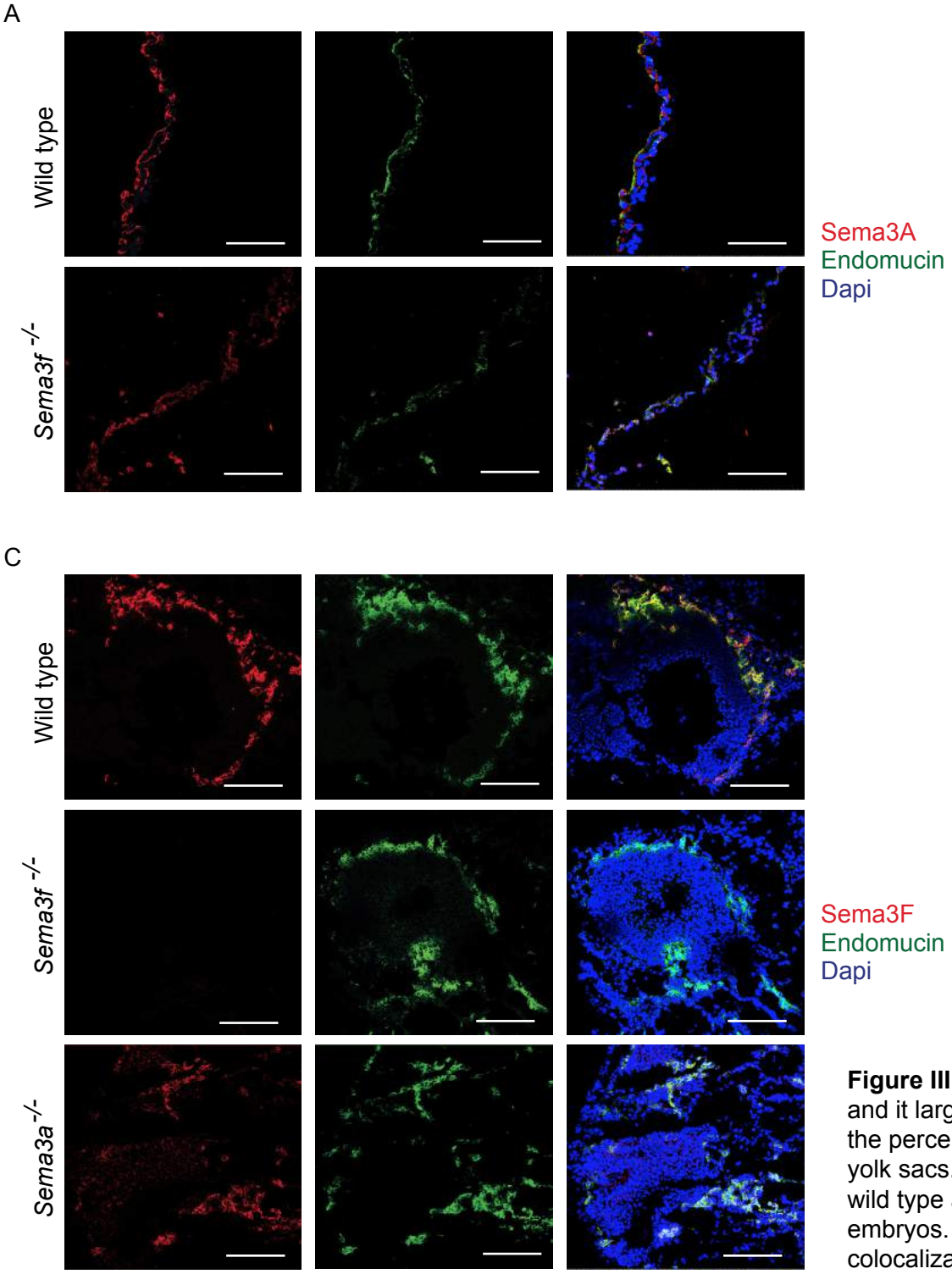

Figure III. A, Sema3 (class 3 semaphorin)-A expression is not affected in Sema3f$^{-/-}$ yolk sacs and it largely colocalizes with endomucin^{+} EnCs (endothelial cells). **B**, Bar graph shows the percentage of Sema3A colocalization with endomucin both in wild type and Sema3f$^{-/-}$ yolk sacs. **C**, In E9.5 embryos, Sema3F is mainly expressed by endomucin^{+} EnCs of both wild type and Sema3a$^{-/-}$ embryos. As expected, Sema3F protein is undetectable in Sema3f$^{-/-}$ embryos. Scale bars, 100 μm. **D**, Bar graph shows the percentage of Sema3F colocalization with endomucin both in wild type and mutant embryos.

Regano_Figure IV

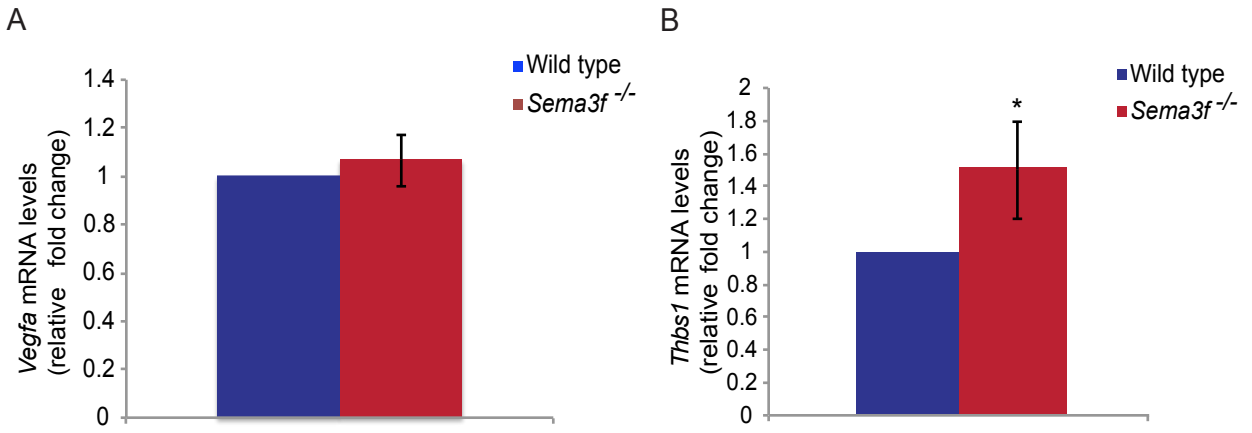

Figure IV. Sema3 (class 3 semaphorin)-F promotes Thbs1 (thrombospondin 1) gene transcription in the mouse yolk sac while does not affect *Vegfa* transcription. **A** quantitative RT-PCR (reverse transcription polymerase chain reaction) on wild type and Sema3f $^{-/-}$ yolk sacs did not display a significant difference in *Vegfa* mRNA transcription level. (n=6). **B** quantitative RT-PCR (reverse transcription polymerase chain reaction) analysis reveals how, compared to wild type yolk sacs, *Thbs1* mRNA increases in Sema3f$^{-/-}$ yolk sacs and decreases in Sema3a$^{-/-}$ yolk sacs (* $p<0.05$).

Regano_Figure V

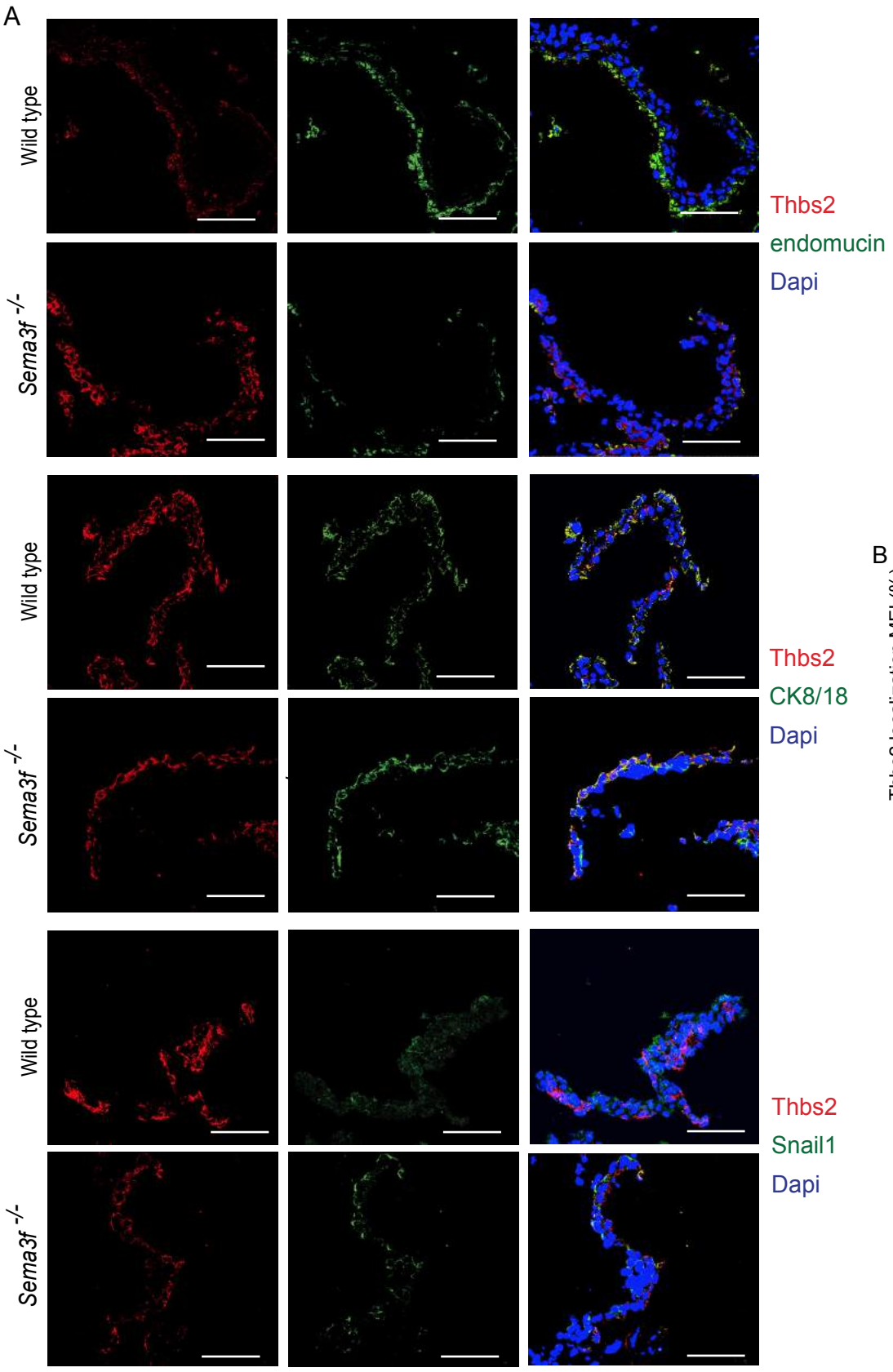

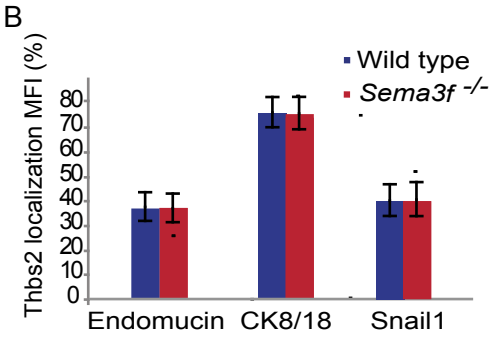

Figure V. Sema3f-knockdown does not affect Thbs2 (thrombospondin 2) protein expression.
A, Quantification of immunofluorescence analysis of E9.5 yolk sacs showed that Thbs2 protein is mainly expressed in CK8/18 (cytokeratin 8/18)$^{+}$ VYS (visceral yolk sac) EpCs (epithelial cells). No differences in Thbs2 expression were observed in Sema3f $^{-/-}$ yolk sacs compared to wild type controls. **B**, Bar graph shows the percentage of Thbs2 (thrombospondin 2) colocalization with endomucin, CK8/18, and Snail1 both in wild type and Sema3f $^{-/-}$ yolk sacs. Scale bars, 100 μm.

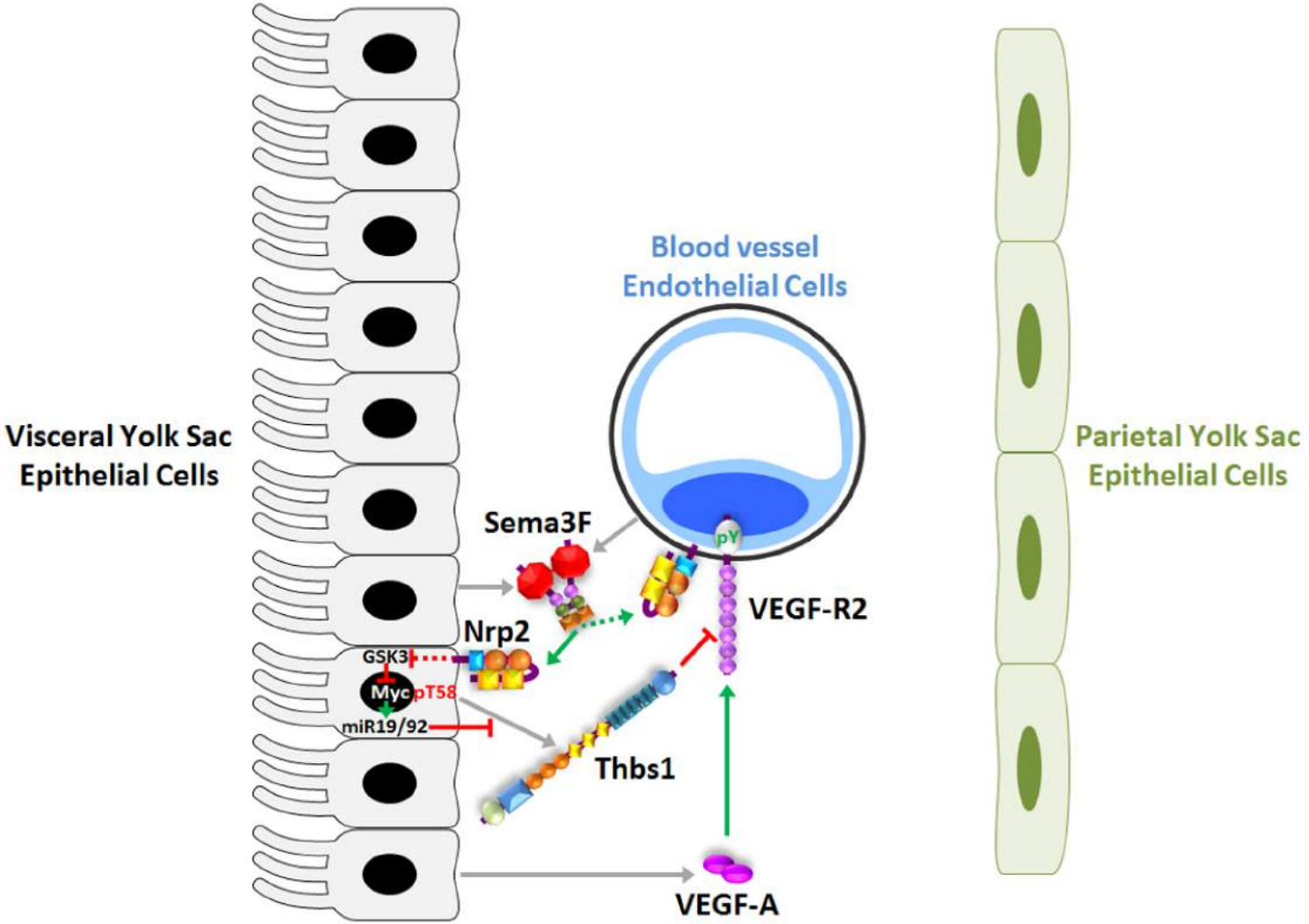

Figure VI. *Semaphorin 3F selectively drives a pro-angiogenic extraembryonic program: a working model.*